博士論文

論文題目　**Sidetrk1 supports the initial outgrowth and branching of the sensory axons by enhancing the transactivation of neurotrophin receptors**　（Sidetrk1は神経栄養因子受容体のトランス活性化を亢進させ感覚神経の初期軸索伸展を支える）

東京大学大学院農学生命科学研究科

水圏生物科学専攻　博士課程

青木　誠

Table of contents

Introduction

Growing axons travel long distances from a cell soma to the target area, guided by environmental cues from target tissues (Dodd and Jessell, 1988; Tessier-Lavigne and Goodman, 1996). Several molecules are reported to affect axon extension either attractive or repulsive manner to form complex neural circuit. Although lots of studies described that the extrinsic factors shape the neuronal circuit in developing neurons, neurons itself retains the ability to shape neurite, a short primary neuronal processes into morphologically and functionally two distinct structures, which are a long protruding process called axon and highly branched processes called dendrite (Dotti et al., 1988). The cascade of phosphorylation increased GSK3β phosphorylation leads to trigger dis-inhibition of proteins called CRMP2 promoting microtubule assembly and makes neurite growth faster and resulted in the axon formation (Yoshimura et al., 2005). This result suggested that cells have already acquired the ability to form distinct structures with endogenous growth promoting mechanisms. Zebrafish primary spinal sensory neurons called Rohon-Beard neurons (RB neurons) have long been served as a good model to study how developing processes obtain a distinct morphology by the mixture of both extracellular and intracellular signaling (Miyashita et al., 2004). RB neurons extend central axon in the spinal cord and peripheral axons in epidermis (Chitnis and Kuwada, 1990; Kuwada et al., 1990). In previous study, peripheral axons of RB neurons extend away from the midline where the repulsive factor Sema3D protein are secreted whereas the central branches of RB neurons did not show any effect by the same proteins (Liu and Halloran, 2005). In contrast, the central axons required TAG-1 protein to extend and form longitudinal fascicles in zebrafish spinal cord and the peripheral axons did not respond to TAG-1 at all (Liu and Halloran, 2005). This study well illustrated the qualitative difference of two distinct processes in terms of response to the same molecule. And it implies mechanisms that establish the qualitative difference of two neuronal processes in the same cell.

Previous study on Islet2a (Isl2a) had been carried out in primary sensory neurons of zebrafish embryos (Segawa et al., 2001). Isl2a plays a crucial role for the

extension of peripheral axons of primary sensory neurons. *isl2a* is a member of *islet* gene family consisting of *islet-1*, *islet-2a* and *islet-2b* in zebrafish (Tokumoto et al., 1995) and the expression patterns were well differentiated among the family members. Islet genes code for the LIM-homeodomain (LIM-HD) transcription factor expressed in post-mitotic neurons to specify motor neuron identity in the developing spinal cord (Thor et al., 1999). LIM-HD proteins contain N-terminal tandem repeats of cysteine-rich regions called the LIM domain and a DNA-binding homeodomain (Dawid et al., 1998). The LIM domains bind to Ldb-1 protein (also called the nuclear LIM interactor, NLI) (Agulnick et al., 1996) and Lhx-3 to form a protein complex that mediates the transcription of specific mRNA (Lee and Pfaff, 2003). During neurogenesis, this complex synergistically induces transcription from HB9 promoters to promote motor neuron differentiation (Lee and Pfaff, 2003). Previous study showed that overexpressing the LIM domains of Isl2a could inhibit the binding to Ldb-1 and thus functionally repress Isl2a (Segawa et al., 2001). As a result, the peripheral axons of zebrafish primary sensory neurons did not extend normally, whereas the central axons remained intact (Segawa et al., 2001). Therefore, it was quite reasonable to expect that factors transcribed by Isl2a signaling might be involved in the extension of peripheral axons, and proposed a model whereby genes transcribed by Isl2a might determine why two axons extend and/or how the polarized growth of axons is achieved. To address this issue, Dr. Segawa, a former researcher of our laboratory, came up the idea that the isolation of whose expression patterns are affected by functional blockage of Isl2a. Accordingly, he took advantage of a transgenic fish model in which GFP expression is specifically activated in sensory neurons to enable their efficient identification and recovery (Higashijima et al., 2000; Uemura et al., 2005). The trigeminal neurons were dissected out and collected using fine glass capillary under a dissecting microscope. Then he pooled an annotated cDNA library of interest and manually selected clones thought to represent rare transcripts that had not been studied in neurons to test their expression in sensory neurons. Finally, he compared gene expression patterns between control and LIM^{Isl2a}-overexpressing embryos. By these relatively laborious procedures, he could isolate novel genes expressed in sensory neurons and examine changes in mRNA expression induced by the functional depression of Isl2a.

This study had started to find the novel gene whose transcription is up- or down-regulated by Isl2a and be involved in the extension of peripheral axons of zebrafish sensory neurons. This thesis consists of two parts. The first part is selecting novel genes isolated by previous work and changed expression by Isl2a. Next approach is asking whether these genes truly involved in the extension of peripheral axons of sensory neurons by knocking-down the translation of encoding proteins using morpholino antisense oligonucleotides. Four Isl2a downstream genes were repressed those protein translations and the axonal extension of examined the extension of peripheral axons of Rohon-Beard (RB) neurons. All genes showed the inhibition of peripheral axon extension in RB neurons. The second part of the thesis reported functional analysis of gene named *sidetrk1*. After the clone selection, I injected morpholino antisense oligonucleotide to find novel molecules supporting the polarized growth of peripheral axons of zebrafish primary sensory neurons. Through this phenotype-driven screening, I could isolate one of candidate genes involved in Isl2a-dependent growth of peripheral axons. Of particular interest, I further studied a Golgi- and endosome-localized membrane protein, Sidetrk1 (Sdtk1), which are also named *tmem59-like*, because it seemed to be involved in the intracellular trafficking of neurotrophin receptor, Trk.

The neurotrohpin signaling is involved in the survival and growth of axons in developing neurons. Neurotrophins are provided by target tissues and bind to their receptor, neurotrophin receptors Trk to send out survival or growth signals (Huang and Reichardt, 2003). Application of neurotrophin to cultured sensory neurons attracts growth cone of neurons. However, cultured trigeminal neurons isolated from early stages of development do not produce neurites in response to nerve growth factor (NGF). Therefore, young neurons could utilize other trophic factors or mechanisms to prevent cell death and maintain their axon elongation by neurotrophin-independent manners. Other neurotrophins, brain-derived neurotrophic factor (BDNF) and neurotrophin 3 (Ntf-3) have been shown to be molecules secreted from both target epithelium and pathway mesenchyme and thereby induced neurite in vitro. However the elimination of both *bdnf* and *ntf-3* genes could not abolish the extension of peripheral axons of trigeminal neurons (Davies, 1994; O'Connor and Tessier-Lavigne, 1999. This

discrepancy between the *in vitro* and *in vivo* data suggested that there might be some other factors or systems to support initial axon extension in developing neurons. Recently, several lines of evidence suggested that Trk is activated by a mechanism called "transactivation" via pituitary adenylate cyclase-activating polypeptide, PACAP-derived signaling in cultured cells, suggesting that neurons could utilize Trk signaling without the action of neurotrophins (Lee et al., 2002; Rajagopal et al., 2004).

In this study, I showed that Sdtk1 plays a key role for the initial outgrowth and branching of axons in developing neurons by the facilitation of the PACAP-mediated transactivation of Trk.

Abbreviations

cDNA: complementary deoxyribonucleic acid

CHAPS: 3-[(3-Cholamidopropyl)dimethylammonio]propanesulfonate

ERK: extracellular signal-regulated kinase

kDa: kilodalton

mRNA: messenger RNA

PBS: phosphate buffered saline

RNA: ribonucleic acid

SDS: sodium dodecyl sulfate

SDS-PAGE: sodium dodecyl sulfate – polyacrylamide gel electrophoresis

Part 1

Screening for genes transcriptionally regulated by Isl2a in zebrafish sensory neurons

Results

1 Selection of cDNAs whose mRNA expression was changed by Isl2a dysfunction

Previous researcher conducted a systematic screen in zebrafish for molecules regulated by Isl2a (Figure 1). First, he created a sensory neuron-derived cDNA library from transgenic fish embryos expressing GFP specifically under control of the sensory neuron-specific enhancer of *islet-1* (Higashijima et al., 2000; Uemura et al., 2005). He determined the cDNA sequence of 3188 individual clones followed by a similarity search in NCBI using the BLASTX algorithm and identified 139 genes not present in the zebrafish EST database and not reported in any species at the time of experiment. Next, he confirmed that 44 of the 139 genes showed mRNA expression in sensory neurons using 24 hours post-fertilization (hpf) zebrafish embryos. Of these, 26 genes showed changed mRNA expression with overexpression of the dominant-negative form of Isl2a (Table 1) (Segawa et al., 2001), with all but one showing reduced or diminished mRNA expression and the remaining gene showing increased expression (Table 1). These 26 genes were therefore regarded as possible downstream targets of Isl2a.

2 *simplet*, *tppp*, *tusc5*, and *sdtk1* clones are possible Isl2a downstream genes

The 26 clones showed changes in mRNA expression in the LIM^{Isl2a}-overexpressing embryos, with several already implicated in axon extension or the developing nervous system. This suggested that our screening could be effective to isolate genes involved in inhibiting axon extension in sensory neurons with LIM^{Isl2a} overexpression. Next, I selected four genes from our screening that have no reported function in axon growth to identify novel genes involved in Islet-2a-dependent axon extension.

The first such candidate gene, *simplet,* is homologous to human *fam53b* (Thermes et al., 2006). This gene encodes no functional protein domains and its exact molecular function has not been determined. *simplet* was mainly expressed in the

central nervous system and also in muscle cells. Knocking down of *simplet* caused delayed epiboly formation and reduced body size, suggesting a role in cell proliferation (Thermes et al., 2006). Another report implicated *simplet* in fin regeneration of zebrafish (Kizil et al., 2009). In the 24 hpf zebrafish embryo studied herein, *simplet* was expressed in trigeminal neurons, cranial ganglion cells, and a subset of hindbrain neurons (Figure 2A). In spinal cord, *simplet* transcripts were found in Rohon-Beard (RB) sensory neurons (Figure 2B), and in Islet-2a dominant-negative embryos, the mRNA expression of *simplet* was significantly reduced in both spinal cord and trigeminal neurons (Figure 2E and 2F).

The second novel gene candidate is *tppp*, which is homologous to human *tubulin polymerization promoting protein (tppp)*. This protein was isolated from bovine brain (Takahashi et al., 1991) and later found to promote polymerization or stabilization of microtubule (Tirian et al., 2003; Tokesi et al., 2010). In wild-type zebrafish embryo, the *tppp* was expressed in trigeminal neurons (Figure 2C), spinal neurons including RB neurons, and primary motor neurons (Figure 2D). In non-neural tissue, the *tppp* transcript was found in intestine (Figure 2D). In contrast, the Isl2a dominant-negative embryos showed no *tppp* expression in any tissue or cell type (Figure 2G and 2H).

The third gene selected for study was *tusc5*, a homologue of the human tumor suppressor candidate 5 protein (*tusc5*) gene. *Tusc5* expression is missing in lung cancer patients due to a chromosomal deletion (Konishi et al., 2003). This gene codes for the CD225 domain-containing protein, which has been associated with interferon-induced cell growth suppression (Deblandre et al., 1995). *Tusc5* is expressed in adipose tissue and somatosensory neurons, it is downregulated by cold stimulation, and its expression increases with adipocyte maturation and augmented PPAR gamma signaling. (Koide et al., 2007; Oort et al., 2007). In zebrafish embryos, the *tusc5* gene was expressed in trigeminal and RB neurons as well as hindbrain neurons (Figure 2I and 2J), and the Isl2a dominant-negative embryos showed slightly reduced mRNA expression of *tusc5* in trigeminal and RB neurons (Figure 2M and 2N). Interestingly, the *tusc5* expression seemed to expand ventrally in the spinal cord of Isl2a dominant-negative embryo (Figure 2N), although the origins of cells ectopically expressing *tusc5* remain unclear.

The final gene candidate is *sdtk1,* which encodes the homolog of a gene called

brain-specific membrane-anchored protein (BSMAP) (Elson et al., 1999). There is no known functional domain in this protein, although it has been associated with a membrane protein predicted by the TMHMM membrane protein prediction program. *sdtk1* mRNAs were abundant in both central and peripheral nervous system, while the trigeminal, anterior commissure, diencephalic, hindbrain, cranial, and RB neurons expressed *sdtk1* (Figure 2K and 2L) in 24 hpf embryos. In Isl2a dominant-negative embryos, *sdtk1* mRNA expression was decreased in the anterior commissure, diencephalic, and RB neurons (Figure 2O and 2P), but was not changed in trigeminal and cranial neurons (Figure 2K and 2O).

3 *simplet*, *tppp*, *tusc5,* and *sdtk1* are required for the extension of peripheral axons in Rohon-Beard sensory neurons

RB neurons show bivalent axonal projection, whereby the central axons extend into the spinal cord and the peripheral axons extend toward the body wall of an embryo and are extensively branched to form an arbor structure (Figure 3A and 3B). Axonal trajectories of RB neurons were easily visualized by the immunostaining against acetylated tubulin. Previous study showed that dominant-negative Isl2a inhibits peripheral axon extension. Herein, overexpression of the LIM domains of Isl2a in zebrafish embryo caused selective inhibition of peripheral axon extension in sensory neurons (Figure 3C) as well as axon extension ventrally in primary motor neurons (Figure3D) (Segawa et al., 2001). This accorded with prior expectation that genes transcriptionally regulated by Isl2a could serve in the extension of peripheral axons of sensory neurons. To confirm whether the knockdown of Isl2a downstream genes could affect axon extension in sensory neurons, a reverse genetic approach using morpholino antisense oligonucleotides (MO) had been carried out. MOs against *simplet*, *tppp*, *tusc5,* and *sdtk1* were prepared and injected into one-cell-stage zebrafish embryos. The *simplet*-MO-injected embryo showed stalled extension of the peripheral axons in RB neurons and reduced branching (Figure 3E). Extension of the central axons in RB neurons in the spinal cord did not change, while some primary motor neurons lost axons (Figure 3F, arrow). To measure the complexity of peripheral axons of RB neurons, I then adopted the concept from the sholl-analysis used to quantitate the complexity of

dendritic arbors of neurons by counting the number of crossing points on concentric circles drawn at a given diameter from the soma (see Materials & Method for detail). The numbers of cross points were significantly reduced in the *simplet*-MO-injected embryos (Figure 3M) (control = 28.90 ± 1.36 SEM N = 10; *simplet*-MO = 19.13 ± 2.60 SEM N = 8; $P = 0.0028$, t-test, control vs. *simplet*-MO). The *tppp*-MO also reduced the extension and branching of peripheral axons in RB neurons (Figure 3G and 3M), whereas the phenotype in the central axons was subtle (Figure 3H). Primary motor neurons showed reduced ventral axon extension (Figure 3H) (control = 28.90 ± 1.36 SEM N = 10; *tppp*-MO = 12.00 ± 2.49 SEM N = 8; $P < 0.0001$, t-test, control vs. *tppp*-MO). The *tusc5*-MO reduced the extension of peripheral axons in RB neurons (Figure 3I and 3M) (control = 28.90 ± 1.36 SEM N = 10; *tusc5*-MO = 7.13 ± 0.99 SEM N = 8; $P < 0.0001$, t-test, control vs. *tusc5*-MO). The central axon fascicules were loosened and the extension was slightly reduced (Figure 3J). Finally, the *sdtk1*-MO also reduced the extension of peripheral axons in RB neurons as well as the branching of peripheral axons (Figure 3K and 3M)) (control = 28.90 ± 1.36 SEM N = 10; *sdtk1*-MO = 10.40 ± 1.70 SEM N = 10; $P < 0.0001$. t-test, control vs. *tmem59l*-MO), while the central axons showed only a subtle change. Primary motor neurons extended normally (Figure 3L).

Discussion

In this part, the systemic screening isolated genes whose mRNA levels are changed by Isl2a by comparing the gene expression patterns between wild-type and transgenic embryos. This screening revealed several genes already reported to function in neuronal cells. For example, clone 578 is *drg11*, a paired homeodomain transcription factor expressed in sensory neurons and required for the projection of cutaneous sensory afferent fibers (Chen et al., 2001), while clone 4557 is *fez1*, a homolog of *unc-76* required for normal axon growth and fasciculation in nematode (Bloom and Horvitz, 1997). Several genes have also been implicated in maintaining the structural integrity of neuronal processes such as clone 5884, coding for *map1b*, which plays a role in enhancing microtubule assembly in axons and extension rate in developing neurons (Gordon-Weeks and Fischer, 2000; Tymanskyj et al., 2012). Finally, clone 4055 is *beta-thymosin*, an actin-binding protein that functions in axonal extension in zebrafish

embryonic brain. Antisense-mediated knockdown of *beta-thymosin* caused a defect in midbrain-hindbrain boundary formation as well as neuronal process formation (Roth et al., 1999). These data suggested that the phenotype observed in Isl2a functional repression could result from altered expression of genes regulating axon extension, neuronal differentiation, or neuronal survival. Moreover, this study also isolated four novel genes not previously implicated in axon growth of neurons. Knockdown of each of these genes disrupted peripheral axon extension in RB neurons. Unexpectedly, I found that *simplet* is required for axonal extension in RB neurons. Simplet binds to 14-3-3 adaptor protein and Ski-interacting protein (SKIIP), which are involved in signaling pathways regulating cell proliferation. (Thermes et al., 2006). Thus, Simplet might use different binding partners to execute axon growth in neurons or induce the SKIIP-dependent transcription of genes related to axon growth. Injection of *tppp*-MO decreased axon growth in the expressing neurons. Tppp promotes tubulin polymerization, thus knockdown of Tppp caused decreased polymerization of tubulin polymer that is crucial for proper axon growth (Sakakibara et al., 2013). *tusc5* was also required for axon extension in RB neurons in Isl2a-dependent axon growth. Tusc5 expression was previously localized to somatosensory neurons (trigeminal ganglia and dorsal root ganglion) and may play a role in adipocyte maturation in adult animals. In developing embryo, somatosensory neurons require tusc5 expression to build proper neural networks. Finally, *sdtk1* was found to be also required for axon extension in RB neurons. This is the first report describing a functional role of this gene, although the brain-specific expression of this gene is known. In addition, the deduced protein sequence for expressed *sdtk1* reveals no information regarding functional domains except that it encodes a transmembrane protein. The following part of this thesis reported results of functional analysis of *sidetrk1*.

Part 2

Identification of functional role of *sidetrk1* in the extension of sensory neuron axons

Results

1 Sidetrk1 facilitates the extension and branching of peripheral axons of the zebrafish primary sensory neurons

As discussed above, *Sdtk1* encodes the homolog of a gene called brain-specific membrane-anchored protein (BSMAP) (also known as transmembrane protein 59-like, tmem59l) (Elson et al., 1999) and *sdtk1* mRNA was observed mainly in the primary sensory neurons including Rohon-Beard (RB) neurons (Figure 4A) and trigeminal neurons (data not shown). *sdtk1*-MO injection inhibited both extension and branching of the peripheral axons of RB neurons (Figure 4D, 4H and 4J) compared with the control embryos (Figure 4B, 4G and 4J). The extensions of primary motor neurons were not changed (Figure 4C and 4F, asterisks). In contrast, overexpression of *sdtk1* mRNA caused excessive peripheral axon branching of RB neurons (Figure 4E and 4J). I also performed the rescue of axonal defects caused by the *sdtk1*-MO to confirm the cell autonomy of the effects of the *sdtk1*-MO. By utilizing the multiple protein expression system from a single mRNA using viral 2A peptide, and generated a tandem cDNA construct encoding GFP, 2A peptide and Sdtk1 under the control of the RB neuron specific SSX enhancer (Provost et al., 2007; Uemura et al., 2005). Injection of the *sdtk1*-MO and this rescue construct restored the branching of the peripheral axons of a single RB neuron (Figure 4I), suggesting that Sdtk1 acts cell autonomously to affect the peripheral axon branching and extension.

I conducted a series of control studies to confirm the specificity of the antisense morpholino oligonucleotide. First, I confirmed the effectiveness of the translational blocking of *sdtk1* mRNA by the *sdtk1*-MO by carrying out co-injection of the mRNA encoding Sdtk1 fused with GFP at its C- terminus into the one cell-stage zebrafish embryos. To check the sequence specificity of the *sdtk1*-MO, I introduced silent mutations into the target sequence of the mRNA for this fusion protein and co-injected it with the *sdtk1*-MO in the same manner as above. The *sdtk1*-MO

efficiently abolished the GFP signal from the fusion protein, whereas it did not affect the GFP signal from the mutated fusion protein (Figure 5). This data indicated that the *sdtk1*-MO affected the protein translation in a sequence specific manner. I also used the splicing-blocking MO against the *sdtk1* gene, and obtained the similar level of reduction in the peripheral axons extension in RB neurons (data not shown). To further eliminate the possibility that all these defects were caused by non-specific apoptotic activity of MO, I coinjected the *p53*-MO together with the *sdtk1*-MO. Coinjection reproduced the results of the *sdtk1*-MO injection alone (Figure 6). Injection of both negative control 5-base mis-paired MO and *p53*-MO did not cause any defect in the RB axogenesis (Figure 6). (Provost et al., 2007; Uemura et al., 2005)

2 Neurotrophin receptor signaling is required for peripheral axons extension in RB neurons

In zebrafish embryos, RB neurons express three subtypes of *trk*: *trkA*, *trkB1*, and *trkC1* (also known as *ntrk1, trk2a*, and *ntrk3a,* respectively) (Figure 7A and data not shown) (Martin et al., 1995). The embryos injected with *trkA*-MO showed reduced extension of peripheral axons from RB neurons (Figure 7B), whereas primary motor neurons extended axons (Figure 7C). The similarity of the phenotype caused by *trkA* inhibition to that caused by *sdtk1* inhibition suggested that there is a functional association between *trks* and *sdtk1* in the development of the RB axons. I confirmed whether *trkA*-MO could alter the mRNA splicing of *trkA*. The RT-PCR analysis of mRNA extracted from *trkA*-MO injected embryos showed the amplification of abnormal *trkA* transcript (Figure 8B). The cloning and DNA sequencing analysis revealed that *trkA*-MO successfully blocked the splicing between the 6th exon and the 7th exon of *trkA* mRNA (Figure 8C and 8D). This leads to the premature termination of protein translation of TrkA thereby reducing the functional TrkA protein.

To prove the relationship between Sdtk1 and Trk signaling, the embryos injected with *sdtk1*-mRNA were treated with Trk inhibitor, K252a. *sdtk1*-mRNA could not induce the increased growth of peripheral axons in RB neurons (Figure 7D and 7F). The same phenotype was observed in the embryos treated with the MEK-1 inhibitor, U-0126 (Figure 7E and 7F). These results suggested that Sdtk1 requires Trk kinase

activity and MAPK signaling to affect the arbor structure of RB neurons.

3 Sidetrk1 impairs the cell surface expression of Trk

Coexpression of Sdtk1 with Trks preferentially reduced the amount of high molecular weight TrkA, B1 and C1 protein in the lysate of transfected PC12 cells (Fig. 9A, left panel, closed arrowhead). I performed a pull-down experiment using the cultured cells overexpressing both Sdtk1 and Trks (A, B1 and C1), and found that Sdtk1 bound specifically to the lower molecular weight forms of Trks in the cells expressing both Trks and Sdtk1 (Figure 9B, open arrowhead). There was no difference in the Sdtk1-binding property among different types of Trks (A, B1, and C1) (Figure 9B). I also investigate whether the molecular weight reduction of Trk by co-expression of Sdtk1 was attributable to the differences in the glycosylation state of Trk proteins (Watson et al., 1999). I treated cells expressing Trks using tunicamycin, an inhibitor of N-glycosylation occurring in endoplasmic reticulum and brefeldin A, which disrupts the functional Golgi apparatus. As expected, these inhibitors affected the glycosylation of TrkA protein (Figure 9C). The treatment with brefeldin A induced the shift of the TrkA protein band pattern similar to that as I observed in the Sdtk1 overexpression, while the treatment with tunicamycin shifted the band toward further lower molecular weight (Figure 9C), suggesting that Sdtk1 interferes with the glycosylation of TrkA which should normally take place within the Golgi apparatus.

As the cellular localization of Trks depends on their states of glycosylation (Watson et al., 1999), I next examined the effect of Sdtk1 coexpression on the cell surface expression of Trks. I collected proteins expressed in the plasma membrane by using the Sulfo-NHS-LC-Biotin, which enables to label only the cell surface proteins, and pulled down with Avidin-conjugated beads. Trk proteins were detected using the antibody against HA-tag. The Na+/K+ATPase proteins were used to show the equal protein loading to the gel (Figure 9D). The cell surface expression of Trk was reduced in PC12 cells coexpressing Sdtk1 (Figure 9D, lane 2, 4, and 6 indicated by a closed arrowhead). Sdtk1 was colocalized with Golgi marker, GM130 (Figure 9E) and late endosome/lysosome marker, LAMP2 in Hela cells (Figure 9F). When HA-tagged TrkA alone was expressed in COS-7 cells, TrkA was detected in the surface of cells and the

Golgi apparatus, as shown by the co-localization of GM130 (Figure 10C and 10C'). When Sdtk1 and TrkA were coexpressed, the amount of TrkA in the periphery of cells was reduced and TrkA appeared colocalized with Sdtk1 in the Golgi apparatus and endosomal compartments (Figure 10D and 10D'). Robo1, which failed to bind to Sdtk1, did not change the localization of protein by coexpressing of Sdtk1 (Figure 10E, 10E', 10F and 10F'). I calculated the transportation efficacy and found that the transportation of Trk was about a half of Robo1 in the presence of Sdtk1 (Figure 10A and 10B). I also confirmed that TrkB1 and TrkC1 also colocalized with Sdtk1 in the Golgi apparatus and endosomal compartments (data not shown).

4 Sidetrk1 facilitates transactivation of Trk

The capacity of Sdtk1 to retain Trk in the Golgi and endosomal compartments led the hypothesis that Sdtk1 binds to Trk in order to facilitate the transactivation of Trk which takes place in the intracellular compartment. Previous reports demonstrated that TrkA is phosphorylated via the PACAP signaling. Moreover the activation of Trk is taken place in the Golgi apparatus rather than plasma membrane (Rajagopal et al., 2004). The mechanistic model for transactivation has been reported in several papers since its discovery. PACAP activates GPCR on the cell surface and elicits G protein alpha subunit mobilization that results in the activation of Src (Shi et al., 2010). Finaly the activated Src phosphorylates Trk localized in the Golgi membrane (Shi et al., 2010). PC12 cells were extensively used in the study of neurotrphin receptor signaling as well as PACAP evoked signaling because it expresses PAC1, the PACAP receptors and TrkA (Ravni et al., 2006). And the 615 cells which are derived from PC12 cells and stably overexpresses TrkA (Hempstead et al., 1992) are generally used in the study of PACAP-dependent Trk activation(Rajagopal et al., 2004). I therefore modified the 615 cells to express Sdtk1 and generated two cell lines, the 222 and 2210 cells to see if Sdtk-1 affects the transactivation of Trk. Since PC12 cells differentiate to extend neurites in response to the activation of neurotrophin receptors (Hempstead et al., 1992), I measured the transactivation of Trk by calculating the percentage of differentiated cells in response to the stimulation with PACAP. I confirmed that the overexpression of Sdtk1 facilitates differentiation of the 222 and 2210 cells at the concentration of 5nM

PACAP at which level the 615 cells could not differentiate efficiently (Figure 11D, 11F and 11G). The effect of PACAP was repressed by the addition of the Trk inhibitor K252a, showing that the Trk kinase activity is essential for promotion of cell differentiation by transacivation via PACAP. (Figure 11H).

I next compared the phosphorylation of Trk between 615 and 222 cells stimulated with PACAP. Previous study showed that Trk transactivation occurs in the intracellular compartment. Therefore, I enriched the intracellular pool of TrkA from the cell lysate by depletion of Trk expressed on plasma membrane using biotinylation of cell-surface proteins and the absorption of biotin-tagged proteins (see Materials & Methods). Then the intracellular Trk was immunoprecipitated with Trk antibody to analyze both total amount and phosphorylated Trk. The intracellular Trk increased in the 222 cells as compared to the 615 cells (Figure 11I, IB: Trk). The phosphorylated intracellular TrkA was detected using phosphor-tyrosine (pY) antibody (Figure 11I, IB: pY). The amount of phosphorylated TrkA increased in the 222 cells.

To finally ask whether the reduction of *sdtk1* mRNA could result in reduced transactivation of Trk, I repressed the endogenous expression of the *sdtk1* mRNA in the 615 cells by introducing the short interfering RNA (siRNA) against the *sdtk1* mRNA and observed the differentiation of the 615 cells in response to the PACAP stimulation. To mark the siRNA expressing cells, the GFP expression vector was cotransfected with the siRNA vectors. The negative control siRNA which does not have any sequence complementation in any genes of rat genome database, did not inhibit neurite formation when the cells were stimulated with PACAP (Figure 12B and 12E, arrow). In contrast, I found that the cells expressing the *sdtk1* siRNA1 could not generate neurites efficiently even when they were treated with a high concentration of PACAP (Figure 12D and 12E). I also obtained the same levels of reduction in the efficiency of cell differentiation in response to the PACAP treatment by using two more different siRNAs (Sdtk1-siRNA2 and Sdtk1-siRNA3) which were also targeted against the *sdtk1* mRNA sequence (Figure 12E).

5 RB neurons express PACAP to activate Trk transactivation pathway

The pituitary adenylate cyclase-activating polypeptide type I receptor (PAC1) and vasoactive intestinal peptide receptor (Vipr) both act as receptors for PACAP (Vaudry et al., 2000). *pacap1b, pac1a* and *vipr2* were expressed in RB neurons of 17- and 24-hpf embryos (Figure 13A and 13D, and Figure 14). The embryos injected with *pacap1b*-MO showed defective extension of peripheral axons from RB neurons (Fig. 13C and 13H) compared to control (Figure 13B). In contrast, the *pacap1b*-overexpressing embryos had more extensively branched peripheral axons (Figure 13E and 13I). Coinjection of *sdtk1*-MO with *pacap1b* mRNA caused impairment of the peripheral axon extension in RB neurons (Figure 13F and 13I). Therefore, Sdtk1 activity is required for the conduction of PACAP signaling. Furthermore, in the embryos injected with both *sdtk1* mRNA and *pacap1b*-MO, the extension of peripheral axons was also impaired (Figure 13G and 13H).

6 Sidetrk1 facilitates an initial growth of peripheral axons in RB neurons

I showed that *pacap1b* is expressed RB neurons and required for the extension of peripheral branch. This finding led us to hypothesize that PACAP1 is produced by RB neurons and acts on the same cells to extend peripheral axons. Since the *pacap1b* expression starts from the stage where RB neurons begin to extend peripheral axons, I tested whether Sdtk1 is involved in the axon extension from early stage of RB neuron development. I carried out the time-lapse imaging of RB neurons from 16-hpf to 18-hpf (Figure 15). As expected, control embryo showed axon extension in both central and peripheral axons during the imaging period (Figure 15A-A'' and 15F). At 17-hpf, RB neurons started to form neurites which eventually extended along the body wall to form the peripheral axons (Figure 15A' and 15A''). The *sdtk1*-knockdown embryo failed to extend peripheral axons from 16- to 18-hpf, and the central axons showed slight reduction in the extension (Figure 15B-B'' and 15F). Some peripheral axons once extended outward then showed the retraction in *sdtk1*-MO injected embryo (Figure 15F). Overexpression of the *sdtk1* mRNA could not cause

changes in neurite formation of RB neurons (Figure 15F). Knockdown of *pacap1b* also inhibited the peripheral branch formation (Figure 15C-C'' and 15F). I further tested whether the knockdown of trk receptors expressed in RB neurons affected the initial axon extension.

Knockdown of three Trks (TrkA, B1 and C1) resulted in the inhibition of peripheral branch formation (Figure 15D-D'' and 15F). Knockdown of PACAP receptors showed the decreased neurite formation (Figure 15E-E'' and 15F).

7 Sidetrk1 facilitates the extension of the peripheral axons of the sensory neurons in the dorsal root ganglion

Later in embryonic development, *sdtk1* mRNA expression is observed in most of neurons in central nervous system, cranial ganglia and the retina (Thisse and Thisse, 2004). I found that the dorsal root ganglion (DRG) neurons expressed *sdtk1* in the 33-hpf embryos (Figure 16A). In the *Tg(neurogenin1:GFP)* embryos, the axons of DRG neurons are observed to extend both peripherally and centrally (Figure 16B) (McGraw et al., 2008). However *sdtk1*-MO inhibited the extension of these axons (Figure 16C, 16D and Figure 17). The peripheral axons were by far more often affected than the central axons (Figure 17).

Disucssion

From above results, I could show that Sdtk1 promotes the initial extension and branching of peripheral axons both in RB and DRG neurons by facilitating the PACAP-PAC1-directed phosphorylation of Trk (Figure 18). Sdtk1 facilitates PACAP dependent Trk phosphorylation through the retention of Trk within the intracellular compartment. Sdtk1 selectively activates MAPK signaling and promotes the peripheral axon extension and branching in RB neurons. This autocrine activation pathway plays an important role for the axonal growth of the sensory neurons at the stages when their axons have not reached enough close to the neurotrophin source.

The role of Trk transactivation mechanism in neurons

Recently, it has been reported that transactivation of TrkB by PACAP in cultured hippocampal neuron causes fragmentation of Golgi apparatus and that both Trk activity and MAPK pathway are required for the fragmentation (Schecterson et al.). In addition, the scattered fragments of Golgi apparatus in the neuronal processes are demonstrated to facilitate the dendritic growth and branching (Horton et al., 2005; Ye et al., 2007). These fragmented Golgi apparatus, which is called 'Golgi-outpost', is reported to serve the site for microtubule nucleation to facilitate dendrite branch formation in dendritic arbor neurons of *Drosophila* (Ori-McKenney et al., 2012; Ye et al., 2007). Therefore, I could assume Sdtk1 might facilitate the Golgi fragmentation which would result in increased acentrosomal nucleation of microtubule in the branch point of peripheral axons of RB neurons.

Sdtk1 affects intracellular trafficking of Trk possibly by reducing protein glycosylation

The study using cultured cells revealed that Sidetrk1 reduced surface expressed-Trk and formed incompletely glycosylated Trk. Since the transport of TrkA protein is determined by glycosylation (Watson et al., 1999), non-glycosylated or partially glycosylated TrkA hardly reaches the plasma membrane. This finding is very similar to the recent report suggesting that Tmem59 (a paralogous protein of Sidetrk1) prevents APP protein glycosylation and the transportation to the plasma membrane possibly by reducing *N*- and *O*-glycosylation activity in Golgi apparatus (Ullrich et al., 2010).

The possible roles of Sdtk1 in the adult nervous system

Recently, PACAP was reported to be involved in proliferation of neural stem cell in adult mouse brain and PACAP has a neurogenic effect on neural stem cell both *in vitro* and *in vivo* (Mercer et al., 2004). *sdtk1* is also specifically expressed in the areas of the adult mouse brain such as the hippocampus of dentate gyrus, the cerebellum and the olfactory bulb, spinal cord, and dorsal root neurons according to the Allen Brain Atlas (Lein et al., 2007). It would therefore be interesting to examine whether Sdtk1 also facilitates axonal growth and/or survival of the neurons in these parts of the adult brain.

Acknowledgements

I express my gratitude for every effort to support me to perform this study. Especially, I thank Dr. Hitoshi Okamoto to give me an opportunity to work for such a top-ranked research environment and countless guidance to complete this study. For the revision of thesis, I would like to thank Drs. Shuichi Asakawa, Shigeki Matsunaga, Hideki Ushio and Shugo Watabe. I thank all members of the Okamoto laboratory for their technical assistance, fish care, and helpful discussions. Especially, I thank Dr. Hisaya Kakinuma to critical discussion and valuable suggestions for this study. I would like to thank Drs. David Kaplan and Moses V Chao for the gift of the 615 cell line and Dr. Angus Thomson for correction of the manuscript. The LAMP2 monoclonal antibody was obtained from the Developmental Studies Hybridoma Bank.

Materials & Methods

Fish maintenance and manipulations

Wild-type zebrafish were maintained as described in elsewhere (Westerfield, 2000). Chemical inhibitors were applied as described previously (Hawkins et al., 2008). Antisense morpholino oligonucleotides (MOs) (Gene Tools) against *sdtk1* and *pacap1b*(Wu et al., 2006) were designed to block protein translation of the respective genes, while the MO against *trkA* targeted the sequence between the second exon and second intron boundary of *ntrk1*. For the negative control for the MO study, *sdtk1*-MO harboring five mismatch bases was designed. The MO against *p53* was prepared as described previously (Robu et al., 2007). For the single cell labeling of RB neuron, the sensory neuron specific enhancer of Islet-1 (SSX), Islet-1 promoter, and the cDNA coding for the monomeric orange fluorescent protein, mKO (MBL) were subcloned into the pTol2 vector (Urasaki et al., 2006). The capped-mRNA for transposase were coinjected with the vector.

Chemical inhibitor treatments of zebrafish embyo

Embryos were incubated at 28.5 ^{o}C. Developmental stages were identified based on Kimmel et al. (Kimmel et al., 1995), and chemical inhibitor was applied as described previously (Hawkins et al., 2008). The MEK-1 inhibitor U-0126 (Promega) was dissolved in 10 mM DMSO, while K252a (Sigma) was dissolved in 100 μM DMSO. Embryos at 6-hpf kept in 12-well plates containing breeding water were treated with the diluted inhibitors.

Construction of a sensory neuron cDNA library using trigeminal ganglion

GFP-expressing trigeminal neurons were dissected from Tg(*SSX-isl1:GFP, rw0145*) transgenic fish (Higashijima et al., 2000; Uemura et al., 2005) embryos using a glass microcapillary. mRNAs were purified and converted into cDNAs to construct a library using the Creator^{TM} SMART^{TM} cDNA Library Construction Kit (Clontech). cDNA sequence was determined using an ABI PRISM 3100 genetic analyzer (Applied Biosystems) and further analyzed by a similarity search in NCBI using the BLASTX algorithm.

Injection of antisense morpholino oligonucleotides and capped RNA

Antisense morpholino oligonucleotides (MOs) (Gene Tools) against *simplet, tppp, tusc5*, and *tmem59l* were designed to block protein translation of the respective genes. MO sequences were as follows: *simplet*-MO: CAACACACATCTTTGCCACGGTCCA, *tppp*-MO: TATTTCACCCGAACCCTCAGCCATG, *tusc5*-MO: TCCGTATCTGTGTTTACTGCCATTG, *tmem59l*-MO: ACCCTGCCGCCGAACTGGAGCATCT. MOs were dissolved in double-distilled water and microinjected by air pressure into 1 to 2-cell-stage zebrafish embryos as described previously (Segawa et al., 2001).

Histological and image quantification

Whole-mount *in situ* hybridization and immunohistochemistry of zebrafish embryos were carried out as described previously (Chitnis and Kuwada, 1990; Segawa et al., 2001). Immnostaining of cultured cells were performed as described previously (Yoshimura et al., 2005). Branching of peripheral axons was evaluated by counting the number of crossing points of the peripheral branches with the ventral edge of the spinal cord in the 8th-17th somite. Statistical differences were evaluated by using the unpaired t-test and PRISM 5 software (Graph Pad Software). DRG axon extension was evaluated by examining the ventrally extending axons using the z-stack confocal images. For the cell differentiation assay, stained cells were counted if the length of neurites exceeded the diameter of the cell body. Statistical analysis was performed by Two-factor factorial ANOVA. Differences were considered significant for $p<0.05$. Data are expressed as mean + standard error of the mean (SEM).

Antibodies

A pan-Trk antibody (B3), ERK-1 antibody (K23), and Na+/K+ATPase antibody (H-300) was purchased from Santa Cruz Biotechnology. Antibodies recognizing the HA (3F10) and FLAG tags were purchased from Roche and Sigma, respectively. A phosphotyrosine-specific antibody (4G10) was purchased from MerckMillipore. GFP antibody was purchased from MBL.

Cell culture

PC12 cells were maintained in Dulbecco's Modified Eagle's Medium (DMEM) containing 5% fetal bovine serum (FBS) and 10% horse serum supplemented with penicillin-streptomycin solution (Sigma). COS-7 cells and HeLa cells were maintained in DMEM supplemented with 10% FBS and antibiotics solution. The 615 cells, the derivative of PC12 cells stably expressing human-TrkA and a gift from Dr. Moses V. Chao, was maintained by the same medium of PC12 supplemented with 200 μg/ml G418 (Sigma). For all ligand stimulation experiments, cells were serum-starved by washing once with DMEM, and then culturing in DMEM containing a minimal concentration of serum (1% FBS) for at least 8 hours. In stimulation assay, cells were treated with DMEM containing 50 nM PACAP-38 (Sigma). Transfections were carried out using Lipofectamine™ 2000 (Invitrogen) and 4 μg of plasmid DNA in 6-well plates that were seeded with 6 x 10^5 cells 1 day prior to transfections. The maintenance of cells and cell surface protein biotinylation were performed as described in previously (Rajagopal et al., 2004). Transfections were carried out using Lipofectamine™ 2000 (Invitrogen). The 222 and the 2210 cells were generated by the stable transfection of the *p3xFLAG-human-sidetrk1* plasmid into 615 cells.

Generation of the 222 and the 2210 cells

The 222 and the 2210 cells were generated by the stable transfection of the *p3xFLAG-hs_sidetrk1* plasmid vector. The 615 cells were transfected with the *p3xFLAG-hs_sidetrk1* encoding human Sdtk1 with three tandem FLAG epitope tags added at its C-teminus of protein. After the transfection, cells were selected using the medium containing 200 μg/ml Zeosin (Invitrogen) and the survived colonies were collected and used for this study.

Transient knockdown of *sdtk1* in 615 cells

The siRNA sequences for sidetrk1 were determined by web-based program (http://sirna.wi.mit.edu). The oligonucleotides for siRNA were synthesized and cloned into pSilencer2.1, siRNA expression vector. The vectors were transfected using Nucleofector system (Lonza).

Cell surface protein biotinylation

PC12 cells were transfected with zebrafish *trkA*-HA cDNA with or without zebrafish *sdtk1*-HA. Following the transfection, cells were washed in PBS containing 1 mM $CaCl_2$ and 0.5 mM $MgCl_2$ and treated with 0.5 mg/ml Sulfo-NHS-LC-Biotin as described previously (Rajagopal et al., 2004). Biotinylation reactions were stopped by two washes in PBS containing 0.1 M glycine. Cell lysates were then prepared and incubated with Immobilized NeutrAvidin agarose resin (Thermo Scientific), and bound protein was analyzed by SDS-PAGE followed by immunoblotting.

Intracellular Ntrk1 pooling

The 615 and the 222 cells were seeded onto collagen-I coated fish (Iwaki). Cells were stimulated by treating with 50 nM PACAP-38, and then surface proteins were biotinylated as indicated above. Cell lysates were prepared and the surface proteins were removed by immunoprecipitation with Neutravidin-agarose beads twice. The resulting supernatant was enriched for intracellular TrkA, which was then pulled down using an anti-pan-Trk antibody and Protein A-agarose beads. The pull-downs were analyzed by SDS-PAGE followed by immunoblotting with an anti-phosphotyrosine antibody and anti-pan-Trk antibody.

Immunoprecipitation and immunoblotting

Cells were washed once in Dulbecco's PBS (Sigma) and suspended in lysis buffer (1% Triton X-100, 10 mM CHAPS) supplemented with Complete Protease Inhibitor Cocktail (Roche) and PhosSTOP Phosphatase Inhibitor Cocktail (Roche). Lysates were immunoprecipitated overnight at 4℃ with Protein-A agarose beads (Sigma) and antibody as indicated in each Figure. The agarose beads were then washed three times using lysis buffer. Proteins were separated on 5-20% gradient polyacrylamide gels, and then transferred to polyvinylidene fluoride membranes for immunoblotting. The antibody reaction on the membrane was detected using Western lightning reagent (Perkin Elmer).

Immunofluorescence

For immunostaining, cells on coverslips were fixed in 4% paraformaldehyde for 15 min and rinsed with PBS before permeabilization in PBS containing 0.1% Triton-X100. Permeabilized cells were incubated with 2% blocking reagent (Roche) in PBS containing 0.1% Tween-20. Primary antibodies against the following proteins were used: GM130 (1:250 BD Transduction), LAMP2 (1:50 Developmental Studies Hybridoma Bank), HA (1:250 Roche), and FLAG (1:250 Sigma), pan-Trk (1:250 Santa Cruz Biotechnology). After the primary antibody reaction, cells were rinsed and treated with AlexaFluor-conjugated secondary antibodies (1:500 Invitrogen). Cells were observed by confocal laser scanning microscopy (LSM 510 META, Zeiss) and analyzed using LSM control software (Zeiss).

Chemical inhibitor treatment using Trk expressing cells

PC12 cells were transiently transfected with the expression vector of zebrafish TrkA. Cells were left for 24 hours to obtain maximum protein expression. Inhibitors were treated for 6 hours at the concentration 1ug/ml for Tunicamycin (Sigma) and 50 nM for brefeldin-A (MerckMillipore).

Cell differentiation assay

The 615, the 222 and the 2210 cells were cultured on the collagen-I and poly-D-lysine coated glass cover glass and placed until cells attach to cover glass. Cells were cultured with various concentration of PACAP for 2 days. For cell differentiation assay with K252a treatment, 100 nM K252a (Sigma) was applied to culture medium for 30 minutes followed by the 50 nM PACAP stimulation for 1 day. Fixed cells were stained by FLAG and pan-Trk antibodies and observed using confocal microscope. Differentiated cells were counted if the length of neurites exceeded the diameter of the cell body. Statistical analysis was performed by Two-factor factorial ANOVA. Differences were considered significant for $p<0.05$. Data are expressed as mean + standard error of the mean (SEM).

References

Agulnick, A.D., Taira, M., Breen, J.J., Tanaka, T., Dawid, I.B., and Westphal, H. (1996). Interactions of the LIM-domain-binding factor Ldb1 with LIM homeodomain proteins. Nature *384*, 270-272.

Bloom, L., and Horvitz, H.R. (1997). The Caenorhabditis elegans gene unc-76 and its human homologs define a new gene family involved in axonal outgrowth and fasciculation. Proc Natl Acad Sci U S A *94*, 3414-3419.

Chen, Z.F., Rebelo, S., White, F., Malmberg, A.B., Baba, H., Lima, D., Woolf, C.J., Basbaum, A.I., and Anderson, D.J. (2001). The paired homeodomain protein DRG11 is required for the projection of cutaneous sensory afferent fibers to the dorsal spinal cord. Neuron *31*, 59-73.

Chitnis, A.B., and Kuwada, J.Y. (1990). Axonogenesis in the brain of zebrafish embryos. J Neurosci *10*, 1892-1905.

Dawid, I.B., Breen, J.J., and Toyama, R. (1998). LIM domains: multiple roles as adapters and functional modifiers in protein interactions. Trends in genetics : TIG *14*, 156-162.

Deblandre, G.A., Marinx, O.P., Evans, S.S., Majjaj, S., Leo, O., Caput, D., Huez, G.A., and Wathelet, M.G. (1995). Expression cloning of an interferon-inducible 17-kDa membrane protein implicated in the control of cell growth. J Biol Chem *270*, 23860-23866.

Dodd, J., and Jessell, T.M. (1988). Axon guidance and the patterning of neuronal projections in vertebrates. Science *242*, 692-699.

Dotti, C.G., Sullivan, C.A., and Banker, G.A. (1988). The establishment of polarity by hippocampal neurons in culture. J Neurosci *8*, 1454-1468.

Elson, G.C., de Coignac, A.B., Aubry, J.P., Delneste, Y., Magistrelli, G., Holzwarth, J., Bonnefoy, J.Y., and Gauchat, J.F. (1999). BSMAP, a novel protein expressed specifically in the brain whose gene is localized on chromosome 19p12. Biochem Biophys Res Commun *264*, 55-62.

Gordon-Weeks, P.R., and Fischer, I. (2000). MAP1B expression and microtubule stability in growing and regenerating axons. Microscopy research and technique *48*, 63-74.

Hawkins, T.A., Cavodeassi, F., Erdelyi, F., Szabo, G., and Lele, Z. (2008). The small molecule Mek1/2 inhibitor U0126 disrupts the chordamesoderm to notochord transition in zebrafish. BMC Dev Biol *8*, 42.

Hempstead, B.L., Rabin, S.J., Kaplan, L., Reid, S., Parada, L.F., and Kaplan, D.R. (1992). Overexpression of the trk tyrosine kinase rapidly accelerates nerve growth factor-induced differentiation. Neuron *9*, 883-896.

Higashijima, S., Hotta, Y., and Okamoto, H. (2000). Visualization of cranial motor neurons in live transgenic zebrafish expressing green fluorescent protein under the control of the islet-1 promoter/enhancer. J Neurosci *20*, 206-218.

Horton, A.C., Racz, B., Monson, E.E., Lin, A.L., Weinberg, R.J., and Ehlers, M.D. (2005). Polarized secretory trafficking directs cargo for asymmetric dendrite growth and morphogenesis. Neuron *48*, 757-771.

Huang, E.J., and Reichardt, L.F. (2003). Trk receptors: roles in neuronal signal transduction. Annu Rev Biochem *72*, 609-642.

Kimmel, C.B., Ballard, W.W., Kimmel, S.R., Ullmann, B., and Schilling, T.F. (1995).

Stages of embryonic development of the zebrafish. Dev Dyn *203*, 253-310.
Kizil, C., Otto, G.W., Geisler, R., Nusslein-Volhard, C., and Antos, C.L. (2009). Simplet controls cell proliferation and gene transcription during zebrafish caudal fin regeneration. Dev Biol *325*, 329-340.
Koide, H., Shibata, T., Yamada, N., Asaki, T., Nagao, T., Yoshida, T., Noguchi, Y., Tanaka, T., Saito, Y., and Tatsuno, I. (2007). Tumor suppressor candidate 5 (TUSC5) is expressed in brown adipocytes. Biochem Biophys Res Commun *360*, 139-145.
Konishi, H., Sugiyama, M., Mizuno, K., Saito, H., Yatabe, Y., Takahashi, T., Osada, H., and Takahashi, T. (2003). Detailed characterization of a homozygously deleted region corresponding to a candidate tumor suppressor locus at distal 17p13.3 in human lung cancer. Oncogene *22*, 1892-1905.
Kuwada, J.Y., Bernhardt, R.R., and Nguyen, N. (1990). Development of spinal neurons and tracts in the zebrafish embryo. J Comp Neurol *302*, 617-628.
Lee, F.S., Rajagopal, R., Kim, A.H., Chang, P.C., and Chao, M.V. (2002). Activation of Trk neurotrophin receptor signaling by pituitary adenylate cyclase-activating polypeptides. J Biol Chem *277*, 9096-9102.
Lee, S.K., and Pfaff, S.L. (2003). Synchronization of neurogenesis and motor neuron specification by direct coupling of bHLH and homeodomain transcription factors. Neuron *38*, 731-745.
Lein, E.S., Hawrylycz, M.J., Ao, N., Ayres, M., Bensinger, A., Bernard, A., Boe, A.F., Boguski, M.S., Brockway, K.S., Byrnes, E.J.*, et al.* (2007). Genome-wide atlas of gene expression in the adult mouse brain. Nature *445*, 168-176.
Liu, Y., and Halloran, M.C. (2005). Central and peripheral axon branches from one neuron are guided differentially by Semaphorin3D and transient axonal glycoprotein-1. J Neurosci *25*, 10556-10563.
Martin, S.C., Marazzi, G., Sandell, J.H., and Heinrich, G. (1995). Five Trk receptors in the zebrafish. Dev Biol *169*, 745-758.
McGraw, H.F., Nechiporuk, A., and Raible, D.W. (2008). Zebrafish dorsal root ganglia neural precursor cells adopt a glial fate in the absence of neurogenin1. J Neurosci *28*, 12558-12569.
Mercer, A., Ronnholm, H., Holmberg, J., Lundh, H., Heidrich, J., Zachrisson, O., Ossoinak, A., Frisen, J., and Patrone, C. (2004). PACAP promotes neural stem cell proliferation in adult mouse brain. J Neurosci Res *76*, 205-215.
Miyashita, T., Yeo, S.Y., Hirate, Y., Segawa, H., Wada, H., Little, M.H., Yamada, T., Takahashi, N., and Okamoto, H. (2004). PlexinA4 is necessary as a downstream target of Islet2 to mediate Slit signaling for promotion of sensory axon branching. Development *131*, 3705-3715.
Oort, P.J., Warden, C.H., Baumann, T.K., Knotts, T.A., and Adams, S.H. (2007). Characterization of Tusc5, an adipocyte gene co-expressed in peripheral neurons. Molecular and cellular endocrinology *276*, 24-35.
Ori-McKenney, K.M., Jan, L.Y., and Jan, Y.N. (2012). Golgi outposts shape dendrite morphology by functioning as sites of acentrosomal microtubule nucleation in neurons. Neuron *76*, 921-930.
Provost, E., Rhee, J., and Leach, S.D. (2007). Viral 2A peptides allow expression of multiple proteins from a single ORF in transgenic zebrafish embryos. Genesis *45*, 625-629.
Rajagopal, R., Chen, Z.Y., Lee, F.S., and Chao, M.V. (2004). Transactivation of Trk

neurotrophin receptors by G-protein-coupled receptor ligands occurs on intracellular membranes. J Neurosci *24*, 6650-6658.
Ravni, A., Bourgault, S., Lebon, A., Chan, P., Galas, L., Fournier, A., Vaudry, H., Gonzalez, B., Eiden, L.E., and Vaudry, D. (2006). The neurotrophic effects of PACAP in PC12 cells: control by multiple transduction pathways. J Neurochem *98*, 321-329.
Robu, M.E., Larson, J.D., Nasevicius, A., Beiraghi, S., Brenner, C., Farber, S.A., and Ekker, S.C. (2007). p53 activation by knockdown technologies. PLoS Genet *3*, e78.
Roth, L.W., Bormann, P., Bonnet, A., and Reinhard, E. (1999). beta-thymosin is required for axonal tract formation in developing zebrafish brain. Development *126*, 1365-1374.
Sakakibara, A., Ando, R., Sapir, T., and Tanaka, T. (2013). Microtubule dynamics in neuronal morphogenesis. Open biology *3*, 130061.
Schecterson, L.C., Hudson, M.P., Ko, M., Philippidou, P., Akmentin, W., Wiley, J., Rosenblum, E., Chao, M.V., Halegoua, S., and Bothwell, M. Trk activation in the secretory pathway promotes Golgi fragmentation. Mol Cell Neurosci.
Segawa, H., Miyashita, T., Hirate, Y., Higashijima, S., Chino, N., Uyemura, K., Kikuchi, Y., and Okamoto, H. (2001). Functional repression of Islet-2 by disruption of complex with Ldb impairs peripheral axonal outgrowth in embryonic zebrafish. Neuron *30*, 423-436.
Shi, G.X., Jin, L., and Andres, D.A. (2010). Src-dependent TrkA transactivation is required for pituitary adenylate cyclase-activating polypeptide 38-mediated Rit activation and neuronal differentiation. Mol Biol Cell *21*, 1597-1608.
Takahashi, M., Tomizawa, K., Ishiguro, K., Sato, K., Omori, A., Sato, S., Shiratsuchi, A., Uchida, T., and Imahori, K. (1991). A novel brain-specific 25 kDa protein (p25) is phosphorylated by a Ser/Thr-Pro kinase (TPK II) from tau protein kinase fractions. FEBS Lett *289*, 37-43.
Tessier-Lavigne, M., and Goodman, C.S. (1996). The molecular biology of axon guidance. Science *274*, 1123-1133.
Thermes, V., Candal, E., Alunni, A., Serin, G., Bourrat, F., and Joly, J.S. (2006). Medaka simplet (FAM53B) belongs to a family of novel vertebrate genes controlling cell proliferation. Development *133*, 1881-1890.
Thisse, B., and Thisse, C. (2004). Fast Release Clones: A High Throughput Expression Analysis (ZFIN Direct Data Submission).
Thor, S., Andersson, S.G., Tomlinson, A., and Thomas, J.B. (1999). A LIM-homeodomain combinatorial code for motor-neuron pathway selection. Nature *397*, 76-80.
Tirian, L., Hlavanda, E., Olah, J., Horvath, I., Orosz, F., Szabo, B., Kovacs, J., Szabad, J., and Ovadi, J. (2003). TPPP/p25 promotes tubulin assemblies and blocks mitotic spindle formation. Proc Natl Acad Sci U S A *100*, 13976-13981.
Tokesi, N., Lehotzky, A., Horvath, I., Szabo, B., Olah, J., Lau, P., and Ovadi, J. (2010). TPPP/p25 promotes tubulin acetylation by inhibiting histone deacetylase 6. J Biol Chem *285*, 17896-17906.
Tokumoto, M., Gong, Z., Tsubokawa, T., Hew, C.L., Uyemura, K., Hotta, Y., and Okamoto, H. (1995). Molecular heterogeneity among primary motoneurons and within myotomes revealed by the differential mRNA expression of novel islet-1 homologs in embryonic zebrafish. Dev Biol *171*, 578-589.
Tymanskyj, S.R., Scales, T.M., and Gordon-Weeks, P.R. (2012). MAP1B enhances

microtubule assembly rates and axon extension rates in developing neurons. Mol Cell Neurosci *49*, 110-119.
Uemura, O., Okada, Y., Ando, H., Guedj, M., Higashijima, S., Shimazaki, T., Chino, N., Okano, H., and Okamoto, H. (2005). Comparative functional genomics revealed conservation and diversification of three enhancers of the isl1 gene for motor and sensory neuron-specific expression. Dev Biol *278*, 587-606.
Ullrich, S., Munch, A., Neumann, S., Kremmer, E., Tatzelt, J., and Lichtenthaler, S.F. (2010). The novel membrane protein TMEM59 modulates complex glycosylation, cell surface expression, and secretion of the amyloid precursor protein. The Journal of biological chemistry *285*, 20664-20674.
Urasaki, A., Morvan, G., and Kawakami, K. (2006). Functional dissection of the Tol2 transposable element identified the minimal cis-sequence and a highly repetitive sequence in the subterminal region essential for transposition. Genetics *174*, 639-649.
Vaudry, D., Gonzalez, B.J., Basille, M., Yon, L., Fournier, A., and Vaudry, H. (2000). Pituitary adenylate cyclase-activating polypeptide and its receptors: from structure to functions. Pharmacol Rev *52*, 269-324.
Watson, F.L., Porcionatto, M.A., Bhattacharyya, A., Stiles, C.D., and Segal, R.A. (1999). TrkA glycosylation regulates receptor localization and activity. J Neurobiol *39*, 323-336.
Westerfield, M. (2000). THE ZEBRAFISH BOOK.
Wu, S., Adams, B.A., Fradinger, E.A., and Sherwood, N.M. (2006). Role of two genes encoding PACAP in early brain development in zebrafish. Ann N Y Acad Sci *1070*, 602-621.
Ye, B., Zhang, Y., Song, W., Younger, S.H., Jan, L.Y., and Jan, Y.N. (2007). Growing dendrites and axons differ in their reliance on the secretory pathway. Cell *130*, 717-729.
Yoshimura, T., Kawano, Y., Arimura, N., Kawabata, S., Kikuchi, A., and Kaibuchi, K. (2005). GSK-3beta regulates phosphorylation of CRMP-2 and neuronal polarity. Cell *120*, 137-149.

Figures & Table

Table 1 Summary of sensory neuron-expressed genes identified in a trigeminal neuron library

Clone ID	NCBI Accession number	Gene name	Expression in LIM^{lsl-2} embryo
578	AY753211	*DRG11*	Decreased
1440	XM_695246	*5-HT3A*	Decreased
1616	NM_001128692	*neuroserpin*	Increased
1683	NM_131453	*elavl4*	Decreased
2042	XM_001921007	*similar to Im:6912380 protein*	Decreased
2354	XM_692658	*Leucine zipper, putative tumor supressor 1 (lzts1)*	Decreased
2399	NM_001002507	*neuritin 1*	Decreased
2677	XM_690005	*wu:fj40g07*	Decreased
3766	NM_001007187	*simplet/FAM53b*	Decreased
3884	NM_131872	*vimentin*	Increased
4010	XM_682834	*tubulin polymerization-promoting protein family member 3*	Decreased
4053	NM_001017850	*stathmin 1*	Increased
4055	NM_205581	*thymosin, beta*	Increased
4192	NM_00100559	*ataxin 2-binding protein 1*	Decreased
4557	BC059593	*fez1*	Decreased
4792	NM_001017567	*synuclein, gamma a*	Decreased
4900	BC133105	*neurofilament, medium*	Decreased
4901	BC092860	*G protein gamma2 subunit*	Decreased
4964	NM_200718	*calbindin 2, like*	Decreased
5884	AB370232	*microtubule-associated protein 1b*	Decreased
6041	XM_683807	*tusc5*	Decreased
6045	XM_001338873	*transmembrane protein 196*	Decreased
6089	NM_170766	*tlx3b*	Decreased
6343	NM_200601	*paralemmin*	Decreased
6625	AF329730	*adenylate cyclase-activating peptide*	Decreased
7135	NM_213337	*sidetrk1/tmem59l*	Decreased

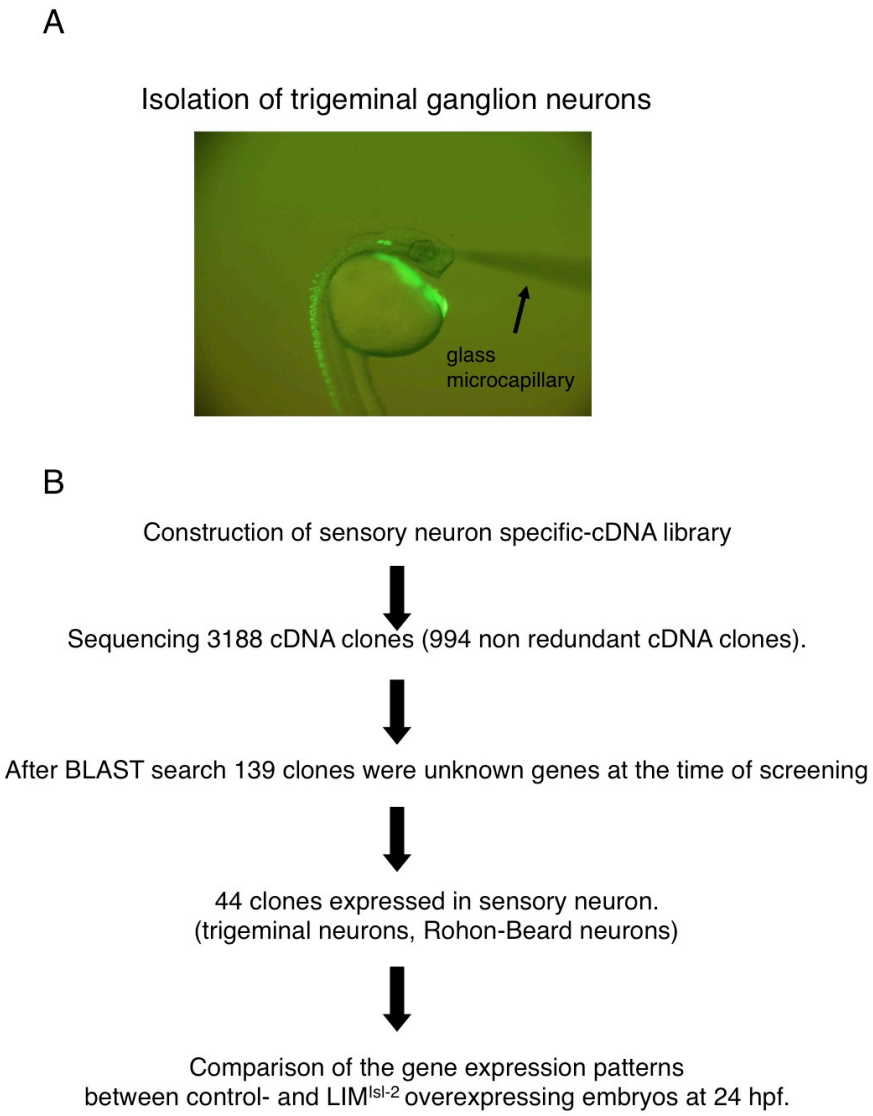

Figure 1 Schematic illustration of Islet2a downstream screening procedure

(A): Collection of trigeminal ganglion neurons with glass microcapillaries. We used *Tg(SSX-isl1:GFP)* transgenic zebrafish expressing GFP in sensory neurons to collect cells from trigeminal ganglion. Using a fine-glass capillary, trigeminal neurons were dissected and collected to construct a cDNA library. (B): Flowchart of the screening procedure. The collected neurons were subjected to mRNA extraction followed by cDNA construction. cDNA clones were sequenced and annotated using the BLAST program, and the expression patterns of selected clones were determined. Genes showing mRNA expression were further analyzed in the embryos expressing LIM^{Isl2a}.

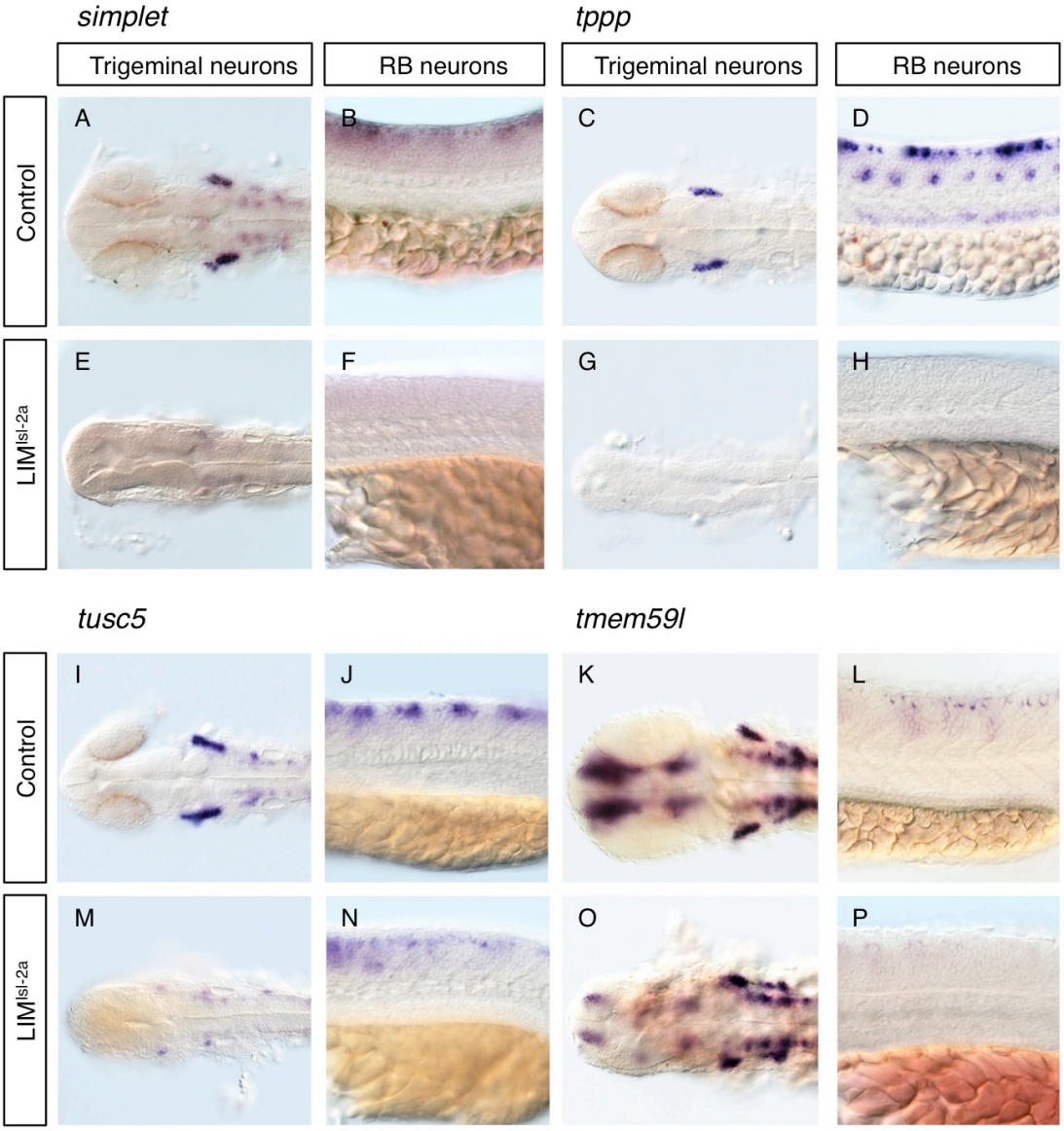

Figure 2: Comparison of gene expression patterns between wild-type and Islet2a dominant-negative embryos

Overexpression of dominant-negative Islet2a reduced the expression of four possible downstream genes. (A, B, E and F) *simplet* mRNA expression pattern in 24 hpf embryo. (C, D, G and H) *tppp* mRNA expression pattern in 24 hpf embryo. (I, J, M and N) *tusc5* mRNA expression pattern in 24 hpf embryo. (K, L, O and P) *tmem59l* mRNA expression pattern in 24 hpf embryo. We compared the gene expression patterns

between control embryos (Control: upper rows, A-D and I-L) and embryos overexpressing the LIM domains of Isl2a (LIM^{Isl2a}: bottom rows, E-F and M-P). We examined the expression of four selected genes in sensory neurons. (A, C, E, G, I, K, M and O) The left lines represent the gene expression patterns in trigeminal sensory neurons. (B, D, F, H, J, L, N and P) The right lines represent the gene expression patterns in RB neurons. Dorsal view (A, C, E, G, I, K, M and O), lateral view (B, D, F, H, J, L, N and P); anterior left, dorsal top.

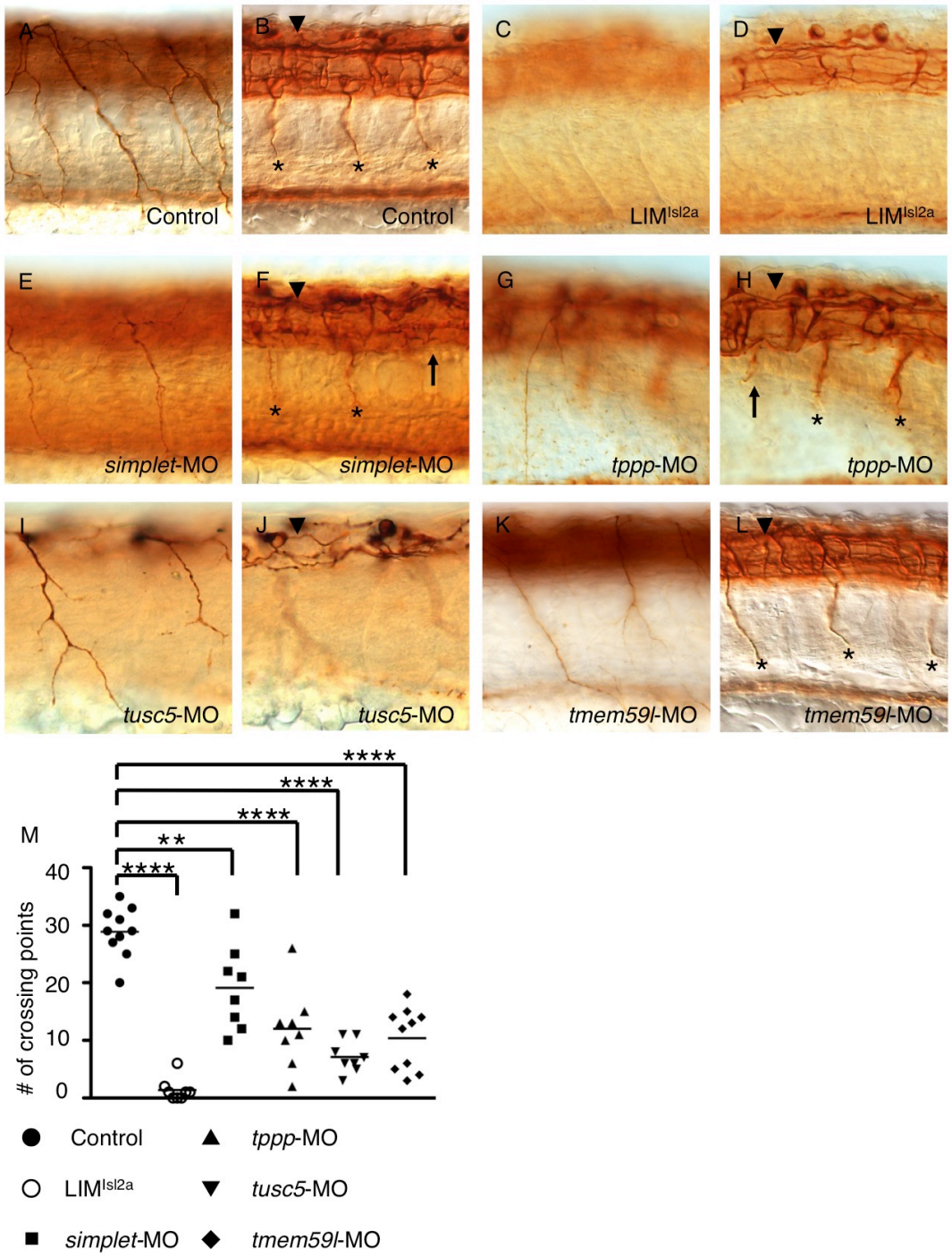

Figure 3 Knock down of possible Islet2a downstream genes inhibits the extension of peripheral axons in Rohon-Beard neurons

Axons of neurons in spinal cord of 24 hpf zebrafish embryos were stained with anti-acetylated tubulin antibody. (A) The peripheral axons of RB neurons extended to

form branched structures. (B) The central axon extended along the longitudinal axis (B, arrowhead), while the axons of primary motor neurons extended ventrally (astarisk) (C) In the embryo overexpressing LIMIsl2a, the peripheral axon extension was disrupted. (D) The central axon extended normally while primary motor neurons could not extend ventral processes. (E) *simlet*-MO reduced the extension of peripheral axons in RB neurons. (F) The central axons were intact in *simplet*-MO-injected embryos and some primary motor neurons did not extend axons ventrally (F, arrow). (G) *tppp*-MO reduced the peripheral axon extension in RB neurons. (H) The central axons showed axon extension, whereas primary motor neuron showed reduced axon extension. (I) *tusc5*-MO reduced the peripheral axon extension in RB neurons. (J) While the central axon extended, primary motor neurons lost their axon extension. (K) *tmem59l*-MO disrupted the extension of peripheral axons in RB neurons. (L) Both central axon and primary motor neurons extended axons normally in the embryos injected with *tmem59l*-MO. (M) Quantitative summary of the MO and Isl2a dominant-negative embryos. The peripheral axons were analyzed by counting the cross points along the line drawn on the ventral edge of spinal cord (see Materials and Methods for detail). (A-L) Lateral view, anterior left, dorsal top. Statistical analysis was carried out by t-test. ****$P < 0.0001$, **$P = 0.0028$

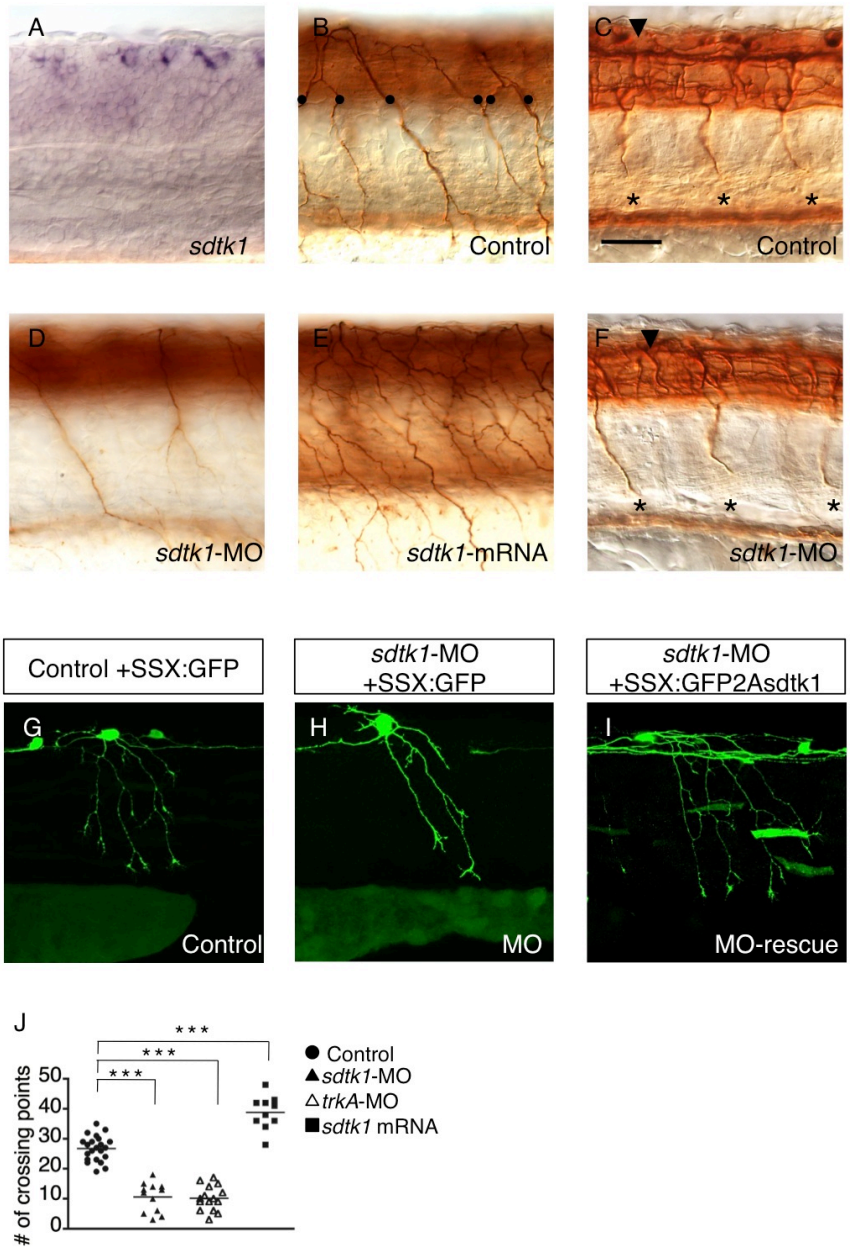

Figure 4 *Sidetrk1 (sdtk1)* expression and its role in peripheral axon development in sensory neurons

(A) *sdtk1* mRNA expression in RB neurons of 24-hpf embryonic spinal cord. (B) In 24-hpf embryos, the peripheral axons of RB neurons extended to form a complex branched structure. The dots indicate the crossing points of RB peripheral axons with the ventral edge of the spinal cord; this number was used for the statistical analysis as in (J) (see Experimental Procedures) (C) In control embryos, the central axons of RB

neurons extended longitudinally (C, arrowhead), while the axons of primary motor neurons extended ventrally (astarisk). (D and F) Injection of *sdtk1*-MO disrupted the extension of the peripheral axons from the RB neurons (D), whereas the central axons remained intact (F, arrowhead). (E) Overexpression of *sdtk1* enhanced branching of the peripheral axons of RB neurons. (G) The stochastic labeling of RB neuron structure by GFP. (H) RB neuron formed less branched peripheral axons in *sdtk1*-MO injected embryo. (I) Overexpression of *sdtk1* in RB neuron recovered from the branching defect caused by *sdtk1*-MO. Embryos were stained by acetylated α-tubulin antibody and images were obtained at the same magnification. Lateral view (A-I), anterior, left (A-I). Scale bar 20 μm (C). (J) Quantification of branching of the peripheral axons of RB neurons. Statistical analysis was carried out by t-test. ***$P < 0.0001$

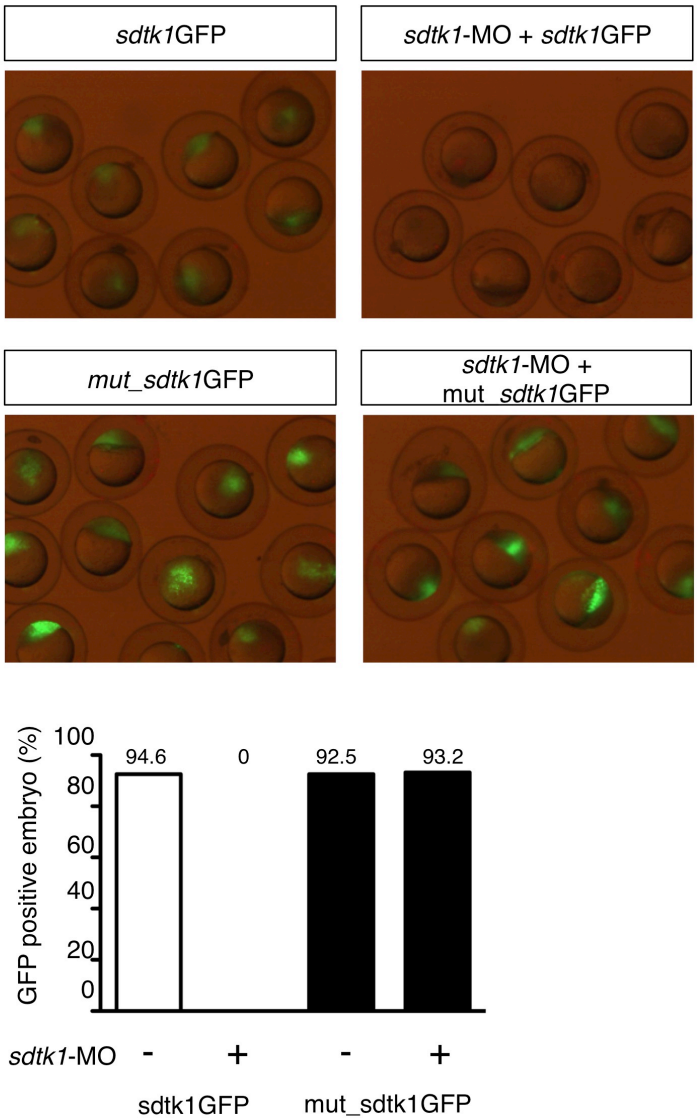

Figure 5 Sequence specific translational blocking of *sdtk1*-MO

In order to verify the specificity of *sdtk1*-MO, we co-injected *sdtk1*GFP fusion mRNA with *sdtk1*-MO. GFP signals disappeared in the embryo injected both MO and sdtk1-GFP mRNA. We prepared mut_*sdtk1*GFP mRNA whose MO targeted sequence were altered to prevent binding of *sdtk1*-MO. Co-injection of mutant GFP mRNA with *sdtk1*-MO caused no changes in GFP signals. All embryos were photographed at 5-hpf. The bar graph also indicated that there are no visible GFP fluorescence in the embryos co-injected *sdtk1*GFP mRNA and *sdtk1*-MO. The value above bars showed the percentage of embryos expressing GFP.

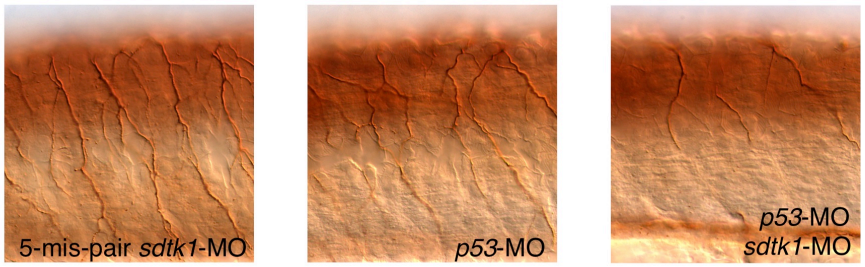

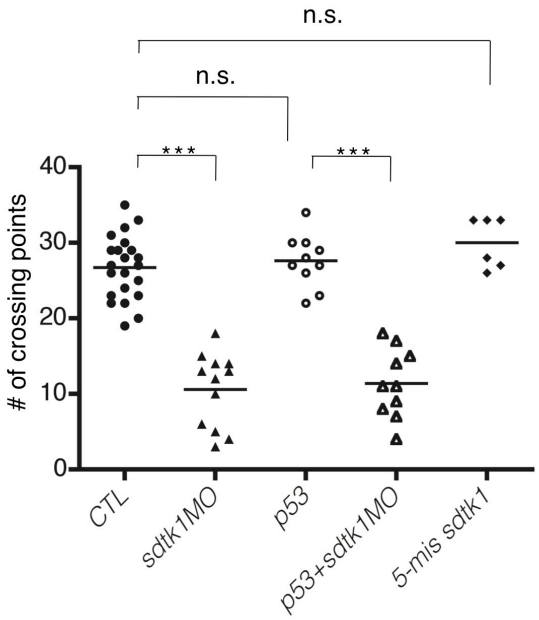

Figure 6 Negative control experiments for *sidetrk1* knockdown study

Control MO having 5 mismatch bases in *sdtk1*-MO was used as the control for MO study. *p53*-MO was injected to avoid the non-specific cell death caused by MO introduction. No obvious effect on the axonal morphology was observed in the embryos injected with *p53*-MO. The *sdtk1*-MO phenotype was not changed by co-injection of *p53*-MO and *sdtk1*-MO. Embryos at 24-hpf were stained by acetylated α-tubulin antibody. And peripheral axon extension was quantified as described in Materials and Methods.

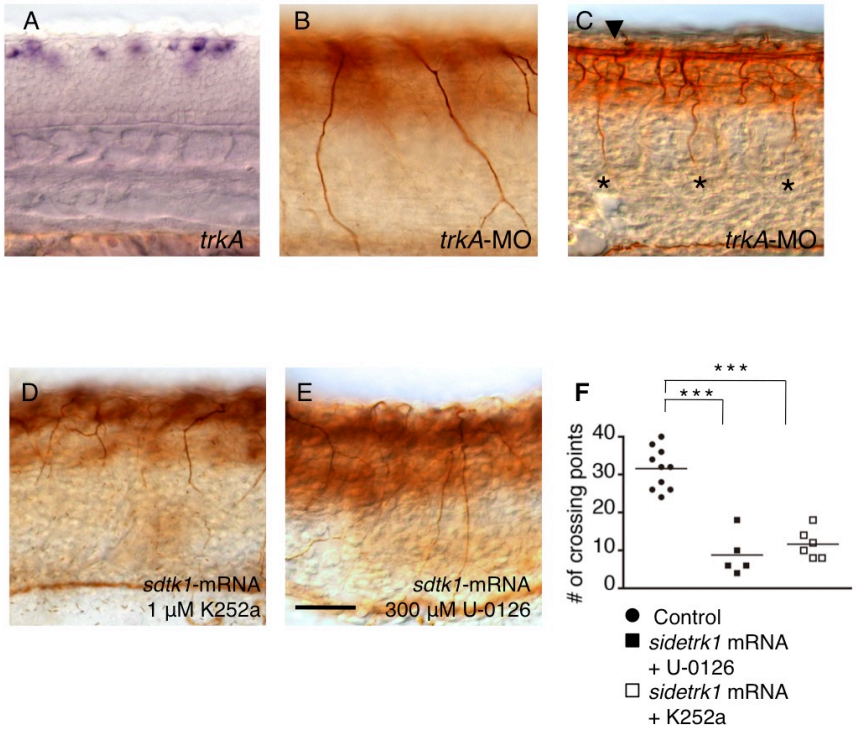

Figure 7 Trk-MAP kinase signaling is required for the extension of peripheral axons in RB neurons of zebrafish embryos

(A) *trkA* expression in RB neurons. (B) Injection of *trkA*-MO reduced extension and branching of the peripheral axons in RB neurons, whereas the central axons remained intact (C, arrowhead). Both Trk kinase activity and MAPK signaling are required for Sdtk1 function. (D) Application of Trk kinase inhibitor (K252a) or (E) MEK-1 inhibitor (U-0126) abolished the excessive branching of peripheral axons caused by *sdtk1* overexpression. (F) Quantification of the peripheral axon branching in RB neurons. Embryos were stained with acetylated α-tubulin antibody and images were obtained at the same magnification. Lateral view (A-E), anterior, left (A-E), dorsal top (A-E). Scale bar, 20 μm (E). Statistical analysis was carried out by t-test. ***$P < 0.0001$

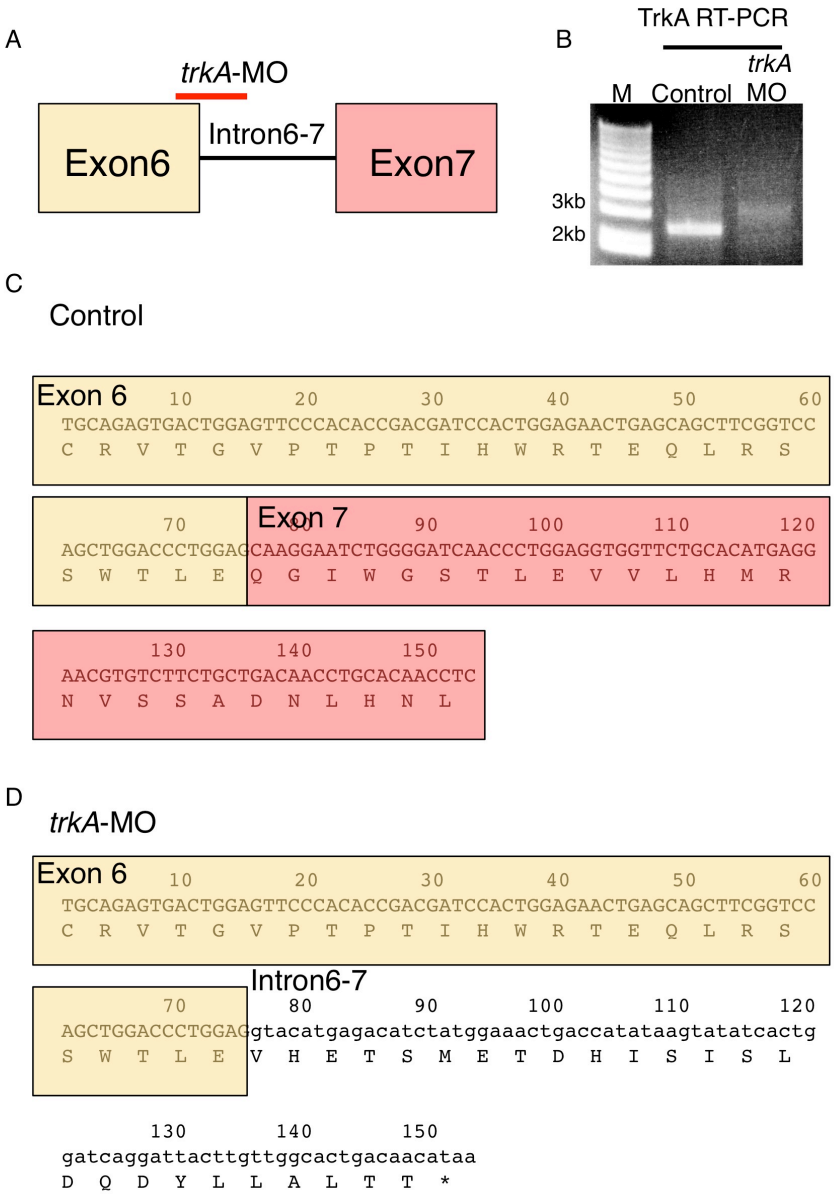

Figure 8 The *trkA*-MO caused abnormal splicing of *trkA* in zebrafish embryo

(A) The *trkA*-MO was targeted at the 6th exon-intron boundary of zebrafish *trkA*. The red line shows the approximate targeted site of MO. (B) RT-PCR revealed abnormal *trkA* transcript in the MO injected embryo. Embryo was injected with MO and subjected to mRNA extraction followed by RT-PCR. (C) DNA senquence of cloned *trkA* cDNA from control animal. (D) DNA sequencing analysis revealed that trkA-MO inhibited mRNA splicing which should be occurred between exon 6 and adjacent intron of *trkA* and resulted in the premature termination of TrkA translation.

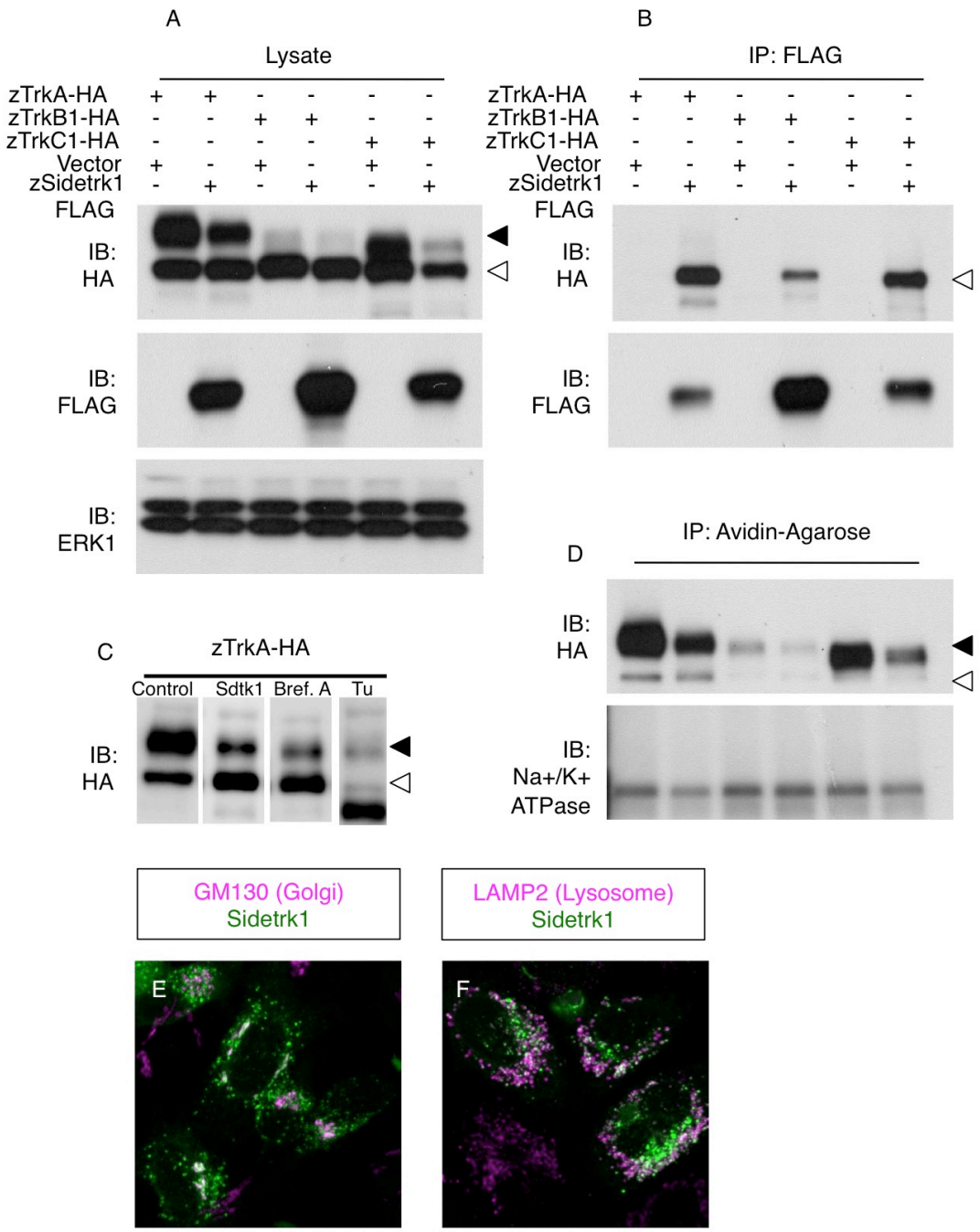

Figure 9 Sdtk1 binds to all subtypes of Trks (TrkA, B1 and C1), and reduces the cell surface expression of Trks

Coexpression of Sidetrk1 and Trks altered the subcellular localization and post-translational modification status of all three Trk proteins. (A) The amount of

high-molecular-weight Trks were reduced by coexpression of Sdtk1 (Lysate blot, lane 2, 4 and 6 closed arrowhead). (B) Sdtk1 bound preferentially to the lower molecular weight forms of Trks (IP: FLAG blot, lane 2, 4 and 6 open arrowhead). (C) The lower molecular weight form of Trk appeared in the Sdtk1 expressing cells (lane 2) corresponds to Trk lacking the glycosylation in the Golgi apparatus. The Brefeldin A (Bref.A, lane 3) treatment inhibited Golgi-dependent glycosylation whereas Tunicamycin (Tu, lane 4) inhibits N-Glycosylation occurred in the ER. Control is the cell expressing TrkA (lane1). (D) Cell surface expressions of Trks were reduced in the cells expressing both Sdtk1 and Trks compared to the cells expressing Trks alone (B, lane 2, 4 and 6). The equal loading of proteins were confirmed by blotting for Na+/K+ ATPase (B). (E and F) Sdtk1 was localized to Golgi apparatus and late endosome/lysosome in HeLa cells expressing zebrafish Sdtk1 fused with the FLAG epitope tag. Transfected cells were fixed and costained with an anti-FLAG antibody and either anti-GM130 antibody (Golgi apparatus) (E) or anti-LAMP2 (late endosome/lysosome) antibody (F).

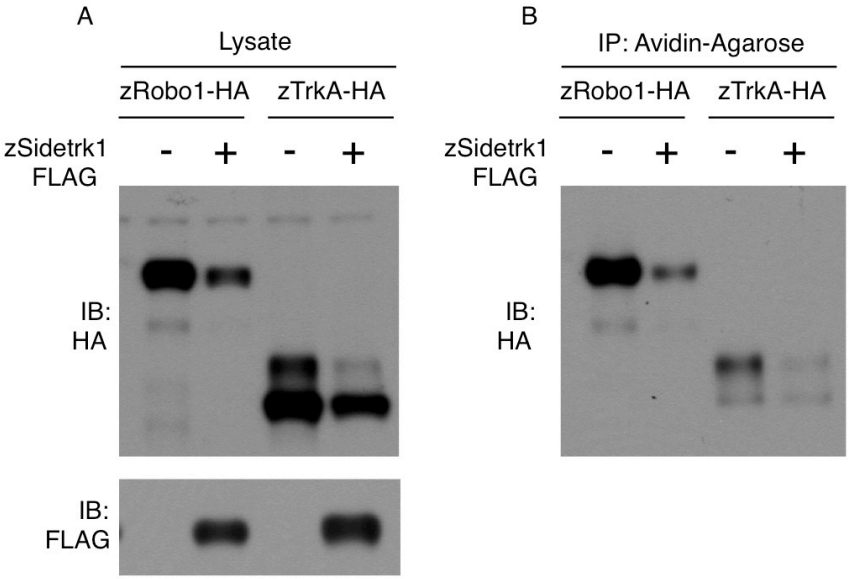

Cell surface expression ratio

Cell surface signal intensity / Lysate signal intensity

	Sidetrk1 (-)	Sidetrk1 (+)
zTrkA	0.412	0.144
zRobo1	0.958	0.640

Normalized cell surface expression score

Sidetrk1(+) expression ratio / Sidetrk1(-) expression ratio

zRobo1 = 0.668

zTrkA = 0.350

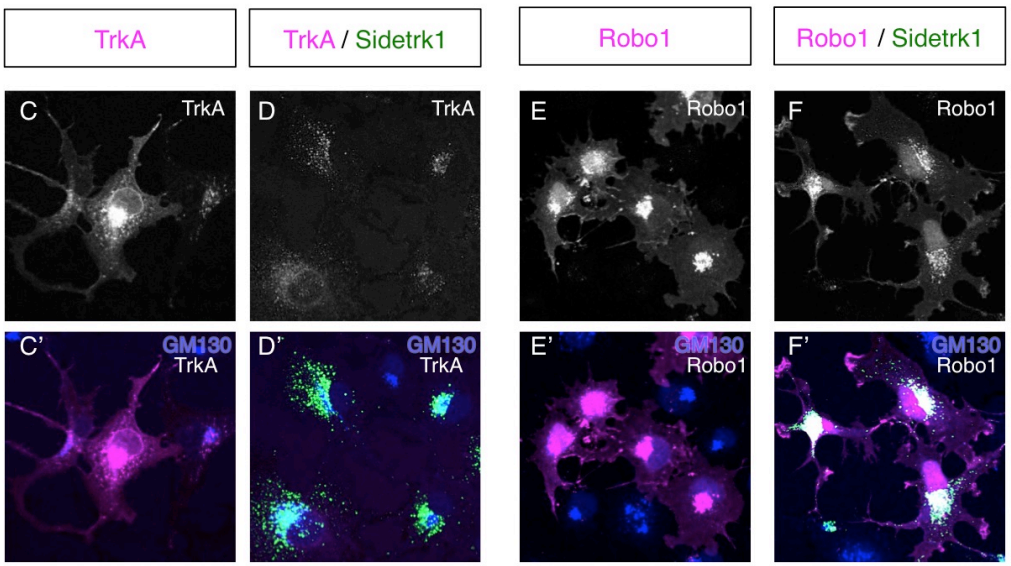

Figure 10 Sdtk1 reduced the cell surface expression of Trk whereas Robo1 which could not bind to Sdtk1 did not change the cell surface protein expression

(A and B) Sdtk1 neither bind to Robo1 nor inhibit the cell surface presentation of Robo1 compared to TrkA. Cell surface expression ratio (SR) showed the efficacy of protein transportation. SR was calculated by dividing the signal intensity of the cell surface protein blot (B) by the signals appeared in the lysate blot (A). Then SR was transformed into the normalized cell surface expression score by dividing the SR of Sdtk1 expressing cells by the SR without the Sdtk1 expression. Finally, Sdtk1 reduced the cell surface expression of TrkA twice more efficiently than Robo1.
(C and C') TrkA was detected in the periphery of the cells expressing TrkA alone. (D and D') Coexpression of Sdtk1 with TrkA reduced the cell surface TrkA and both proteins were colocalized in the Golgi apparatus (blue; labeled by GM130 antibody) and the endocytic vesicles. (E and E') Robo1 was also detected in the cell surface as well as the expression in the intracellular compartments. (F and F') Coexpression of Sdtk1 with Robo1 did not alter the subcellular distribution of Robo1. (C-F) A single channel was extracted from multi-colored immuostaining results. Showing the receptor protein localization. (C'-F') Merged images of stained cells.

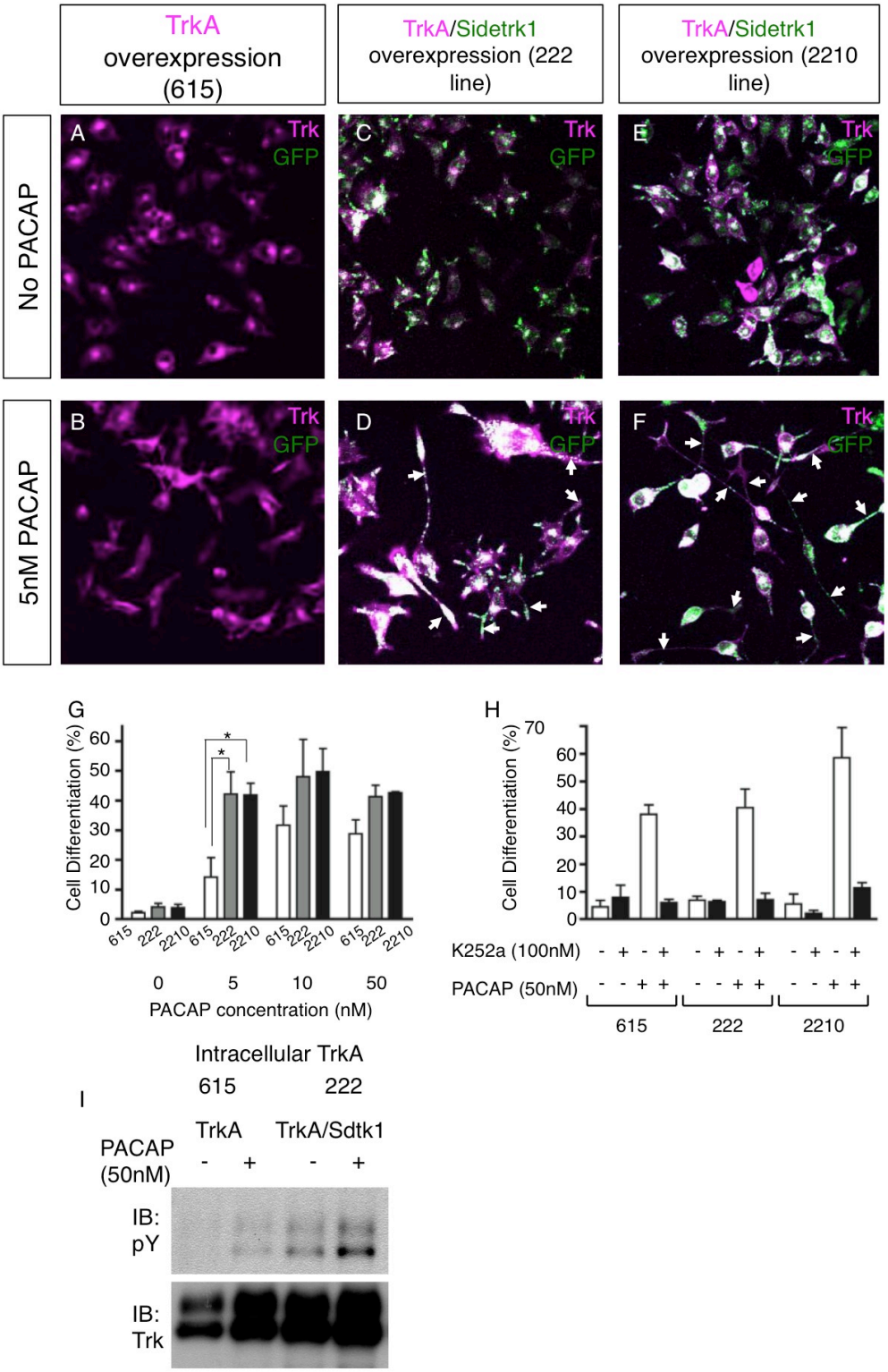

Figure 11 Sidetrk1 facilitates PACAP dependent phosphorylation of Trk

(A-F) Chronic expression of Sidetrk1 enhanced the neurite formation and growth. Neurites extended from soma were indicated by arrows. (B and G) 615 cells, which stably express TrkA, could not extend neurite efficiently. (D, F and G) Sidetrk1 overexpression promoted the differentiation of cells at lower amount of PACAP in both cell lines coexpressing both TrkA and Sdtk1. (H) Trk kinase activity is required for the Sidetrk1-dependent increment of cell differentiation. Inhibition of Trk kinase resulted in the reduction of cell differentiation. (G and H) The data shown are mean ± standard error of the mean (SEM). Statstical analysis was performed by Two-factorial ANOVA. Differences were considered significant for * $P < 0.05$ (I) TrkA phosphorylation in the intracellular compartment following treatment with PACAP was increased by coexpression of Sdtk1. 615 cells expressed TrkA and 222 cells expressed both TrkA and Sdtk1 stably.

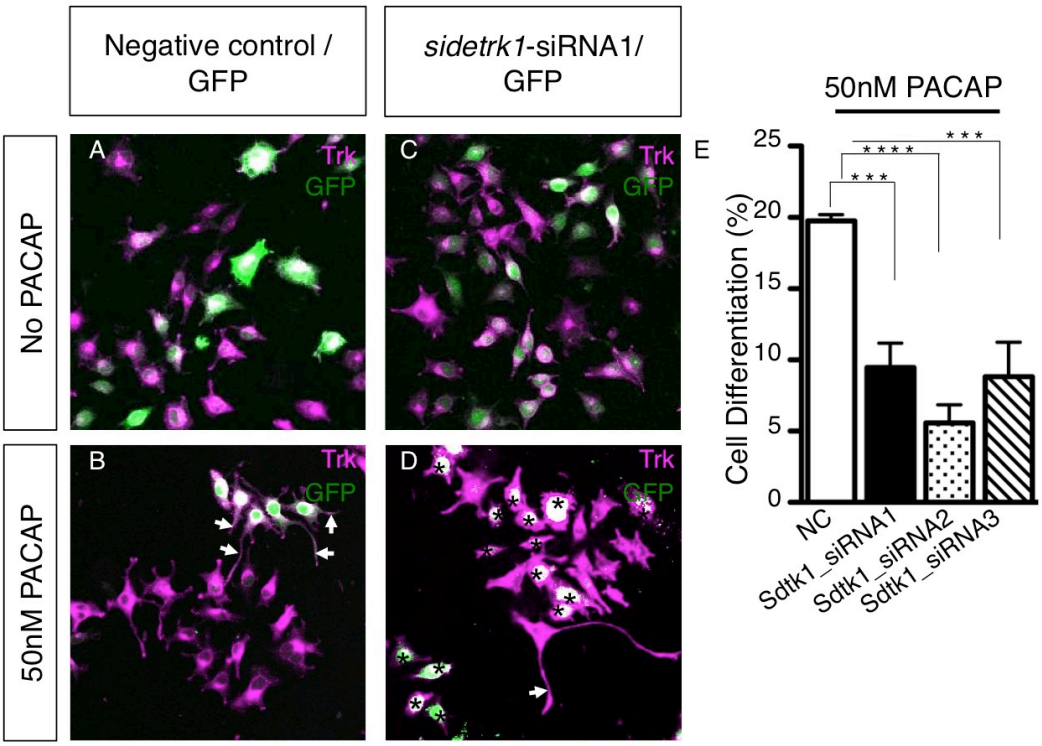

Figure 12 Sdtk1 is required for the PACAP-dependent neurite formation in 615 cells

(A-D) siRNA mediated gene knockdown of *sdtk1* led to inhibition of neurite formation by PACAP stimulation. The GFP expressing vector was cotransfected with the siRNA vector to highlight the siRNA-affected cells. (B) Arrows indicated the elongated neurite by PACAP stimulation. (D) siRNA-affected cells failed to extend neurite in response to PACAP (black asterisks) whereas the siRNA negative cell could formed neurite (white arrow). (E) All the siRNA tested reduced neurite formation. The data shown are mean ± standard error of the mean (SEM). Statstical analysis was performed by Two-factorial ANOVA.

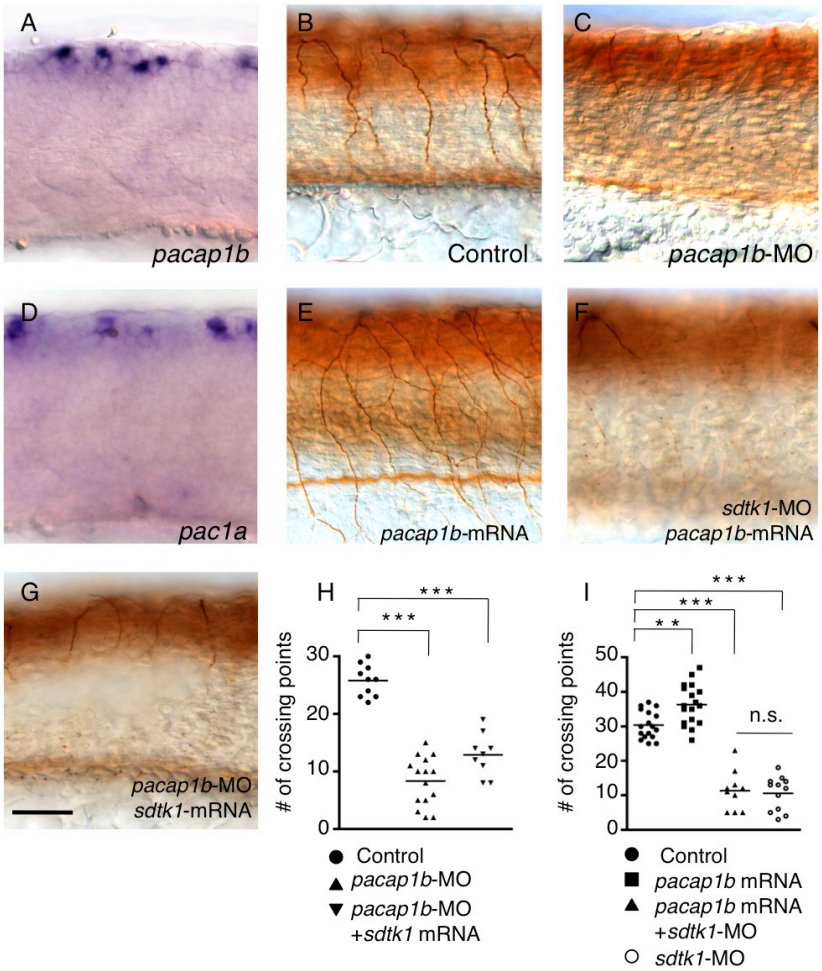

Figure 13 Expression of PACAP1b in RB neurons during early axogenesis and the requirement of PACAP1b signaling for the extension of peripheral axons

(A and D) *pacap1b* and *pac1a* expression in RB neurons of 17-hpf zebrafish embryos. (C) Pacap1b is required for the extension of the peripheral axons in RB neurons. (E) Overexpression of zebrafish *pacap1b* increased the branching of the peripheral axons. (F) Coinjection of *sdtk1*-MO with *pacap1b* mRNA impaired the extension of peripheral axons. (G) Coinjection of *sdtk1* mRNA and *pacap1b*-MO abolished the extension of peripheral axons. Embryos were stained with acetylated α-tubulin antibody and images were obtained at the same magnification. (H and I) Quantification of the peripheral

axon branching in RB neurons. Lateral view (A-G), anterior, left (A-G), dorsal top (A-G). scale bar, 20μm (G). Statistical analysis was carried out by t-test. ***$P < 0.0001$, ** $P < 0.001$

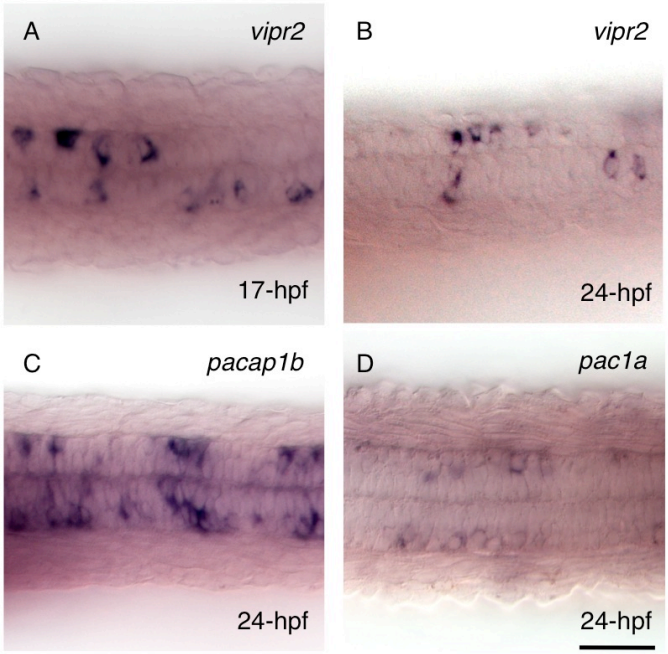

Figure 14 *pacap1b*, *pac1a* and *vipr2* were expressed in RB neurons at 17- and 24-hpf zebrafish embryos

(A and B) *vipr2* was expressed in RB neurons of both 17- and 24-hpf zebrafish embryos. The number of RB neurons expressing *vipr2* and the expression levels of *vipr2* mRNA were higher in the 17-hpf embryos than in the 24-hpf embryos. (C and D) *pacap1b* and *pac1a* were expressed in RB neurons of 24-hpf zebrafish embryos. Dorsal view (A-D), anterior, left (A-D). Scale bar 20 μm (D).

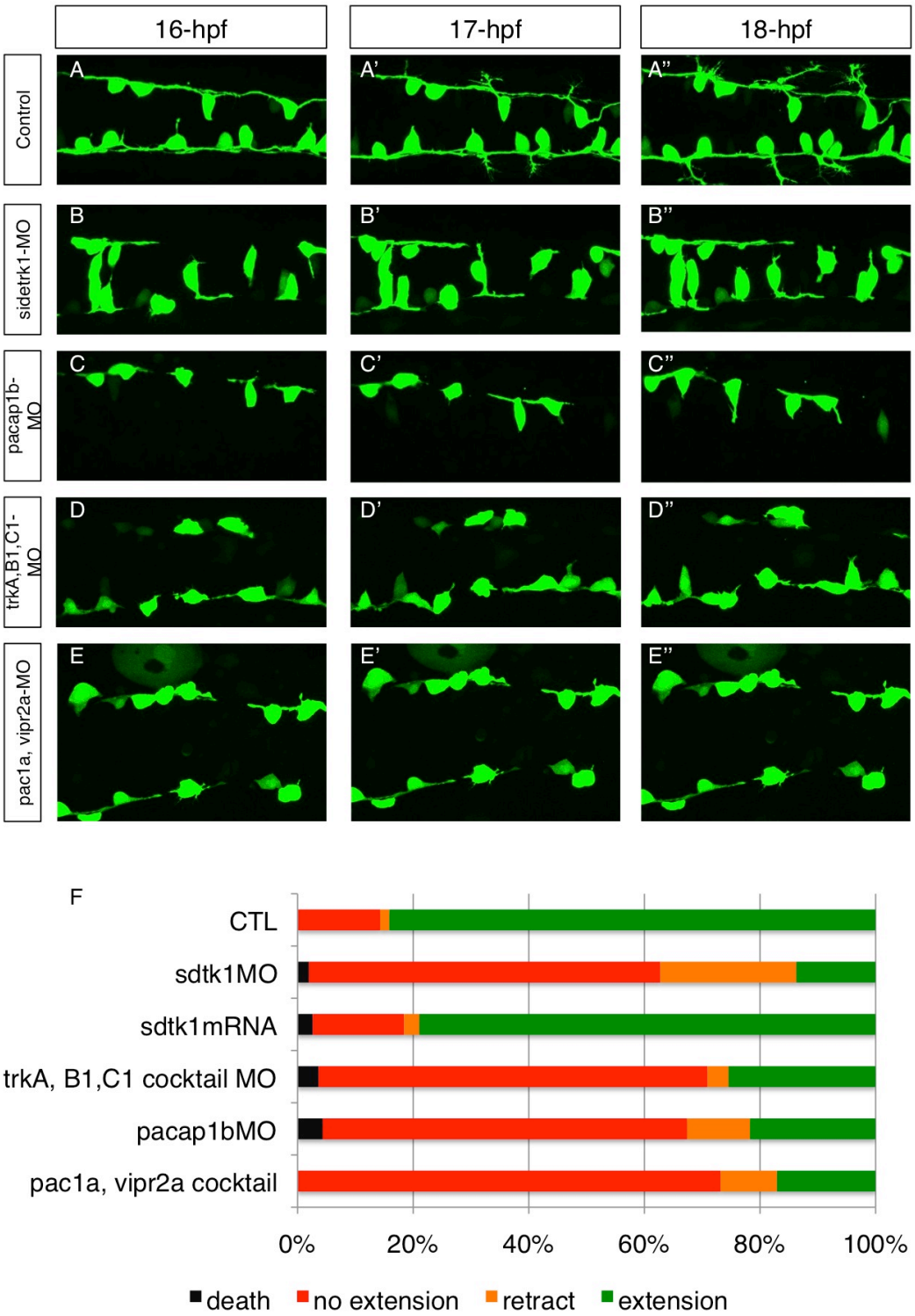

Figure 15 Initial outgrowth of peripheral axons is driven by Trk transactivation

(A-E'') Embryos transiently expressed GFP in RB neruons and injected with MO as described in right side of figure. Live imaging was carried out using agarose-mounted

embryo from 16- to 18-hpf. Dorsal view (A-E''), anterior, left (A-E''). (F) Classification of peripheral axon extension of individual RB neurons during imaging. RB neurons underwent apotosis were classified as 'death'. 'no extension' showed no peripheral axon extension. 'retract' neurons once showed the axonal extension, then stopped and were withdrawn. 'extension' neurons simply showed the peripheral axon extension without any withdrawal behaviors.

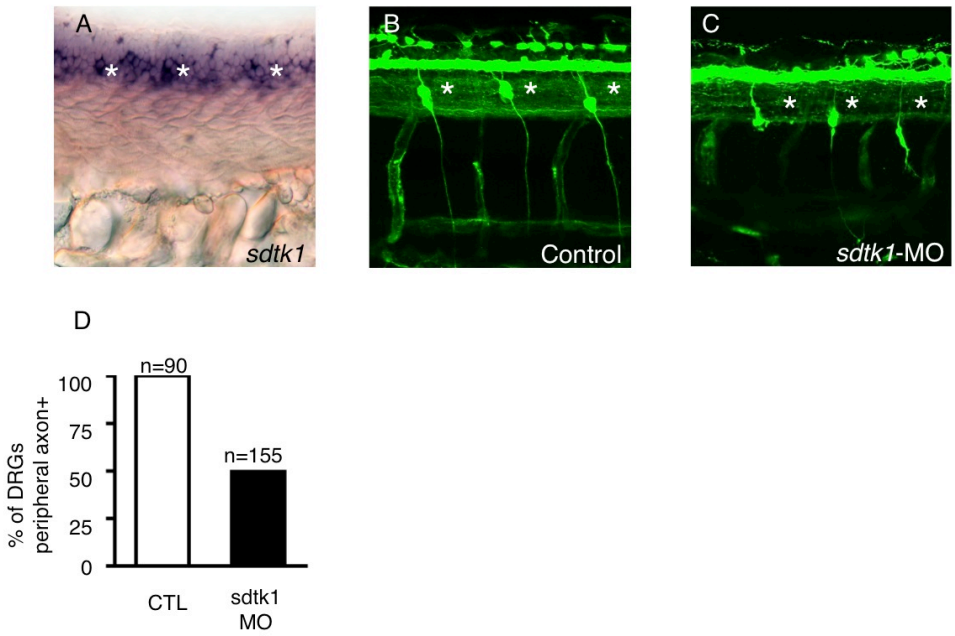

Figure 16 Dorsal Root Ganglion (DRG) neurons require sidetrk1 to extend the peripheral axons

(A) *sdtk1* mRNA expression in DRG neurons of 36-hpf embryonic spinal cord (asterisk). (B) In 3-day post fertilization *Tg(neurogenin1:EGFP)* larva injected with negative control *sdtk1*-MO, DRG neurons extended the peripheral axons normally (asterisk). (C) DRG neurons were defective in extension of the peripheral axons by *sdtk1*-MO injection (asterisk). Embryos were stained by acetylated α-tubulin antibody and images were obtained at the same magnification. Lateral view (A-C), anterior, left (A-C). (D) Percentage of DRG neurons that extended the peripheral axons decreased by *sdtk1*-MO

injection.

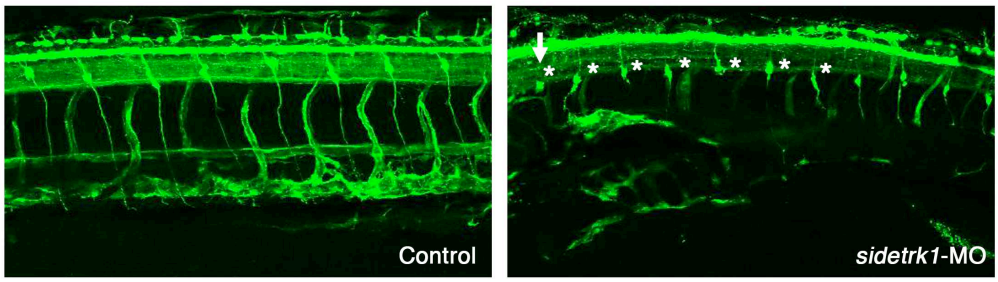

Fig. 17 *sidetrk1* is required for the extension of axons of Dorsal Root Ganglion (DRG) neurons.

sdtk1-MO was injected to the transgenic fish that expresses GFP under the control of *neurogenin1* enhancer. Although injection of *sdtk1*-MO caused the defect predominantly in the extension of peripheral axons of DRG neurons (asterisks, 49.6 %, n=155 neruons), the extension of the central axons of DRG neurons were also affected (arrowheads, 18.7 %, n=155 neurons). Some segments totally lost the DRG neurons (data not shown 2.5%, n=159 segments analyzed). Whereas the control-MO caused almost nothing on the DRG neurons (peripheral axon defects, 2.2%, n=90 neurons, central axon defects, 1.1% n=90 neurons, DRG lost, 1%, n=91 segments analyzed).

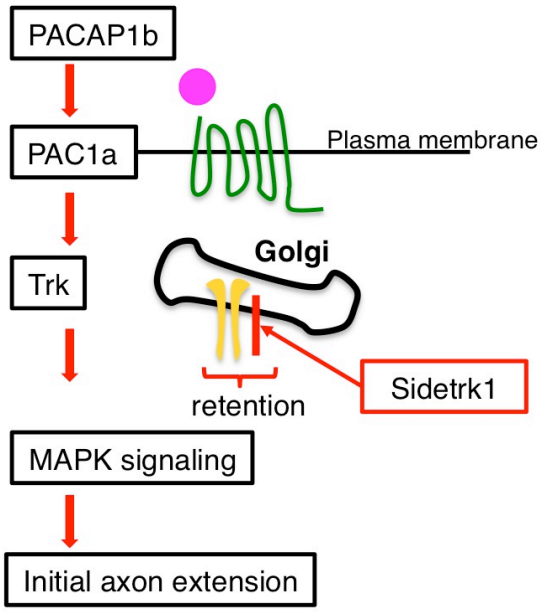

Figure 18 Schematic illustration of Sdtk1 function

Sdtk1 directly binds to Trk and somehow retains it within the Golgi apparatus. This situation is favorable for Trk proteins to receive the phosphorylation signal from PACAP-PAC1 signaling cascade. Therefore Sdtk1 facilitates Trk transactivation.